

One of the subjects in **Chapter 8**:

High energy fragmentation reaction and its importance for galaxy's structure

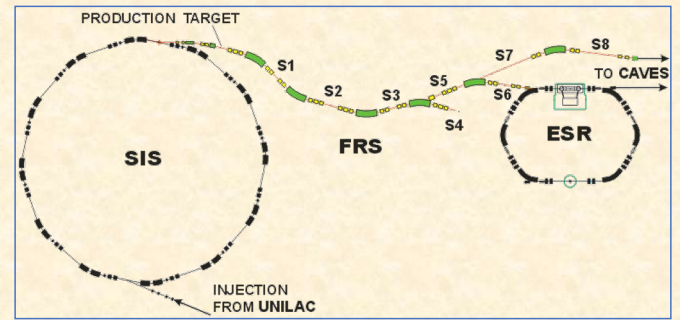
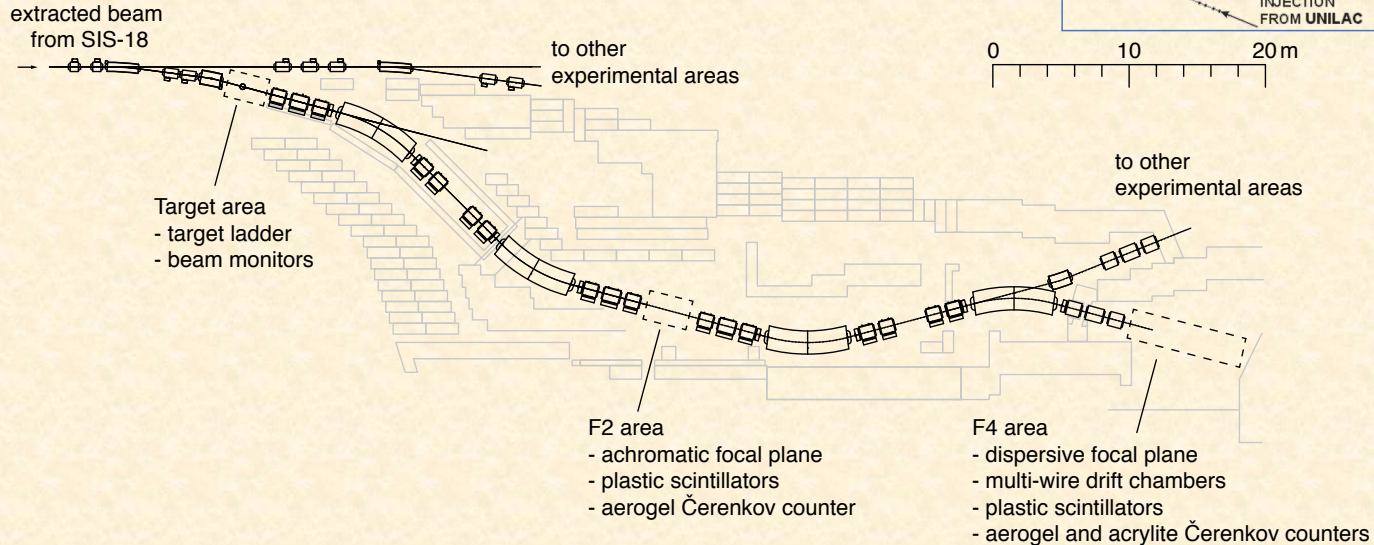
Take R. Saito

- *High Energy Nuclear Physics Laboratory, Cluster for Pioneering Research (CPR), **RIKEN**, Japan*
- *HypHI Group, FRS/NUSTAR department, **GSI Helmholtz Center for Heavy Ion Research**, Germany*
- *Graduate School of Science and Engineering, **Saitama University**, Japan*



*QCD at FAIR Workshop 2024, GSI, Darmstadt, Germany,
11th – 14th November, 2024*

The novel technique with FRS at GSI (2016–)



The novel technique with FRS at GSI (2016–)

extracted beam
from SIS-18
to other
experimental areas

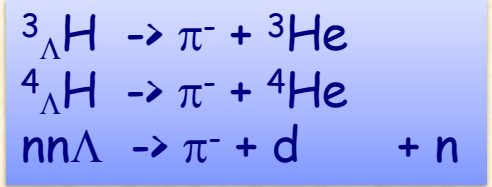
Target area
- target ladder
- beam monitors

F2 area

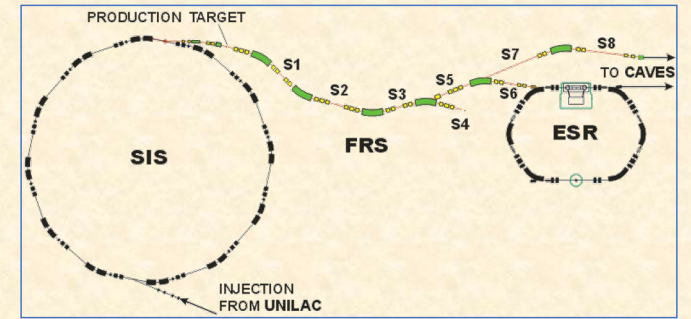
to other
experimental areas

F4 area

- dispersive focal plane
- multi-wire drift chambers
- plastic scintillators
- aerogel and acrylite Čerenkov counters



With ${}^6\text{Li}+{}^{12}\text{C}$ at 2 A GeV



0 10 20 m

INJECTION
FROM UNILAC

TO CAVES

The novel technique with FRS at GSI (2016–)

extracted beam
from SIS-18
to other
experimental areas

Target area
- target ladder
- beam monitors

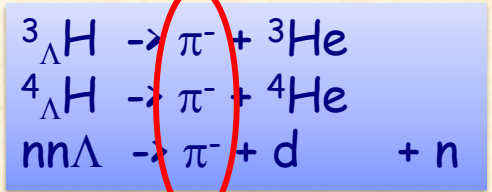
Larger acceptance for π^-
 $\Delta p/p \sim \text{a few \%}$

to other
experimental areas

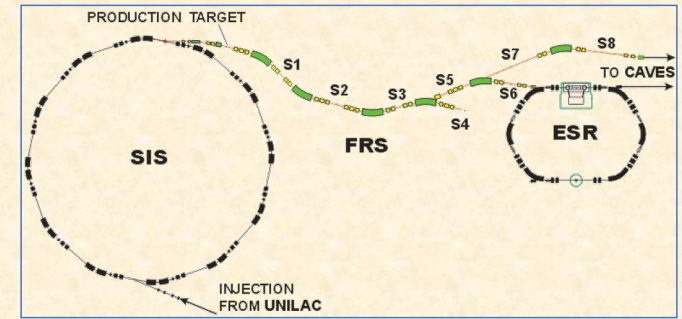
F2 area

F4 area

- dispersive focal plane
- multi-wire drift chambers
- plastic scintillators
- aerogel and acrylite Čerenkov counters



With ${}^6\text{Li}+{}^{12}\text{C}$ at 2 A GeV



The novel technique with FRS at GSI (2016–)

extracted beam from SIS-18
to other experimental areas

Target area
- target ladder
- beam monitors

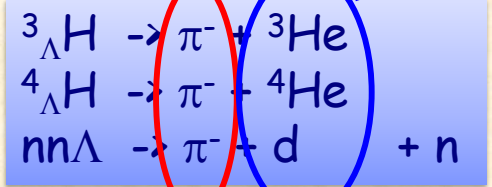
Larger acceptance for π^-
 $\Delta p/p \sim \text{a few \%}$

$\Delta p/p = 10^{-4}$

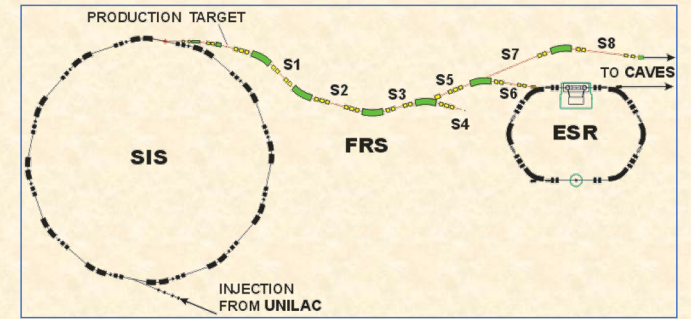
F2 area

F4 area

- dispersive focal plane
- multi-wire drift chambers
- plastic scintillators
- aerogel and acrylite Čerenkov counters



With ${}^6Li+{}^{12}C$ at 2 A GeV



0 10 20 m

to other experimental areas

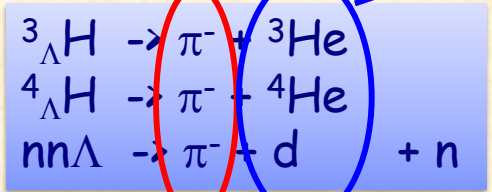
The novel technique with FRS at GSI (2016–)

extracted beam from SIS-18
to other experimental areas

Target area
- target ladder
- beam monitors

Larger acceptance for π^-
 $\Delta p/p \sim \text{a few \%}$

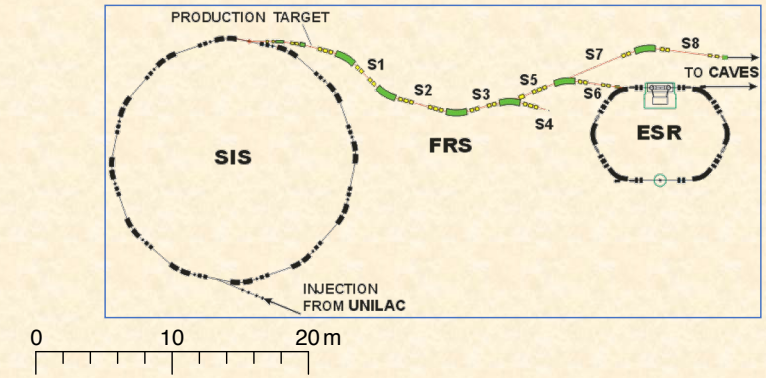
$\Delta p/p = 10^{-4}$



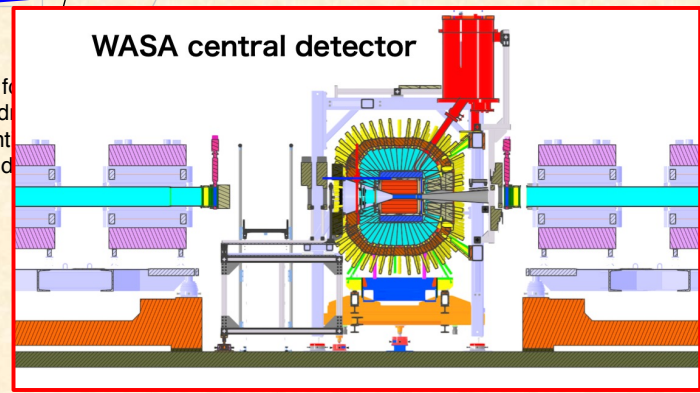
With ${}^6\text{Li} + {}^{12}\text{C}$ at 2 A GeV

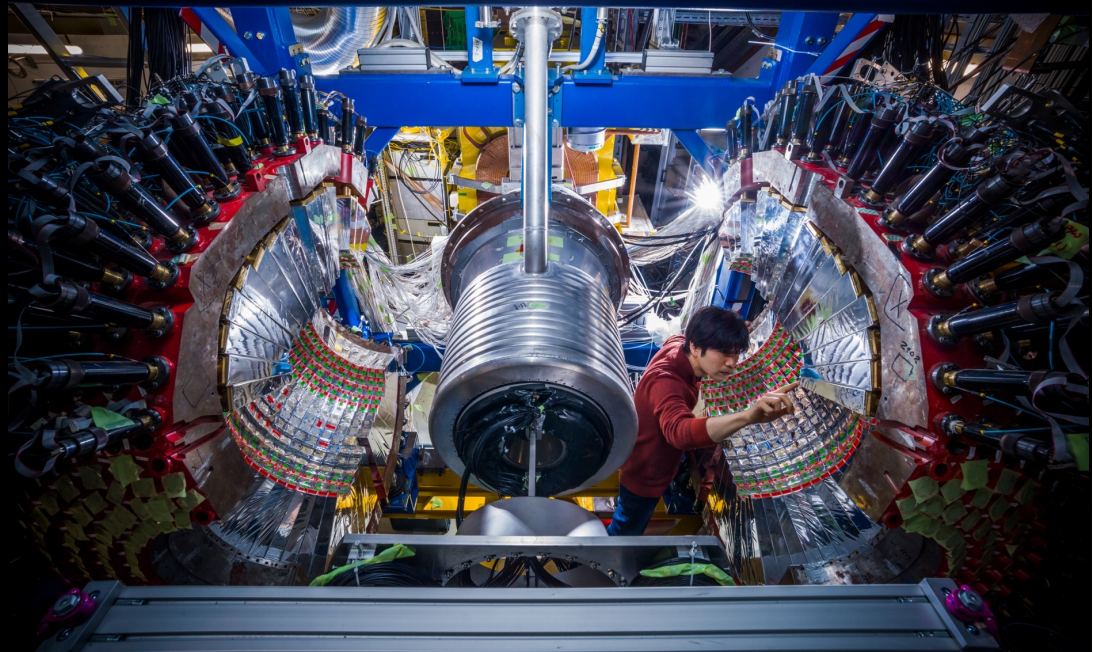
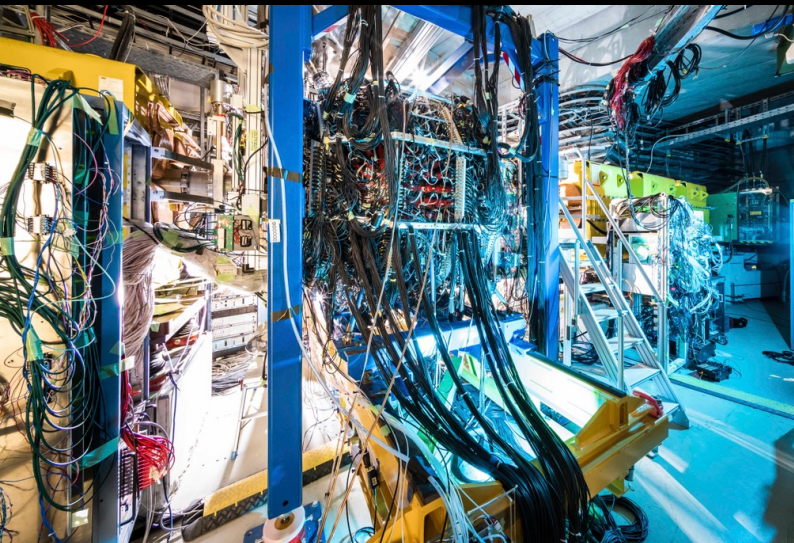
to other experimental areas

Preparation at GSI started in March 2019
Experiment conducted in January-March 2022



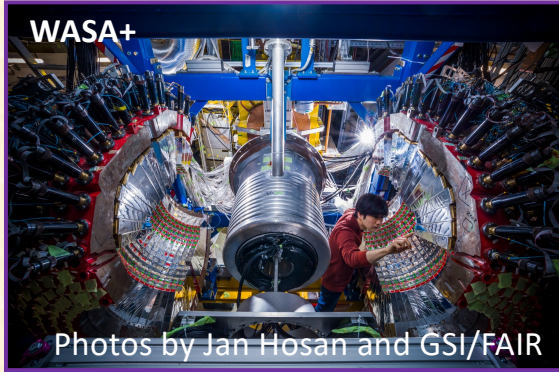
F4 area
- dispersive fo
- multi-wire d
- plastic scint
- aerogel and





Photos by Jan Hosan and GSI/FAIR

Our wishes



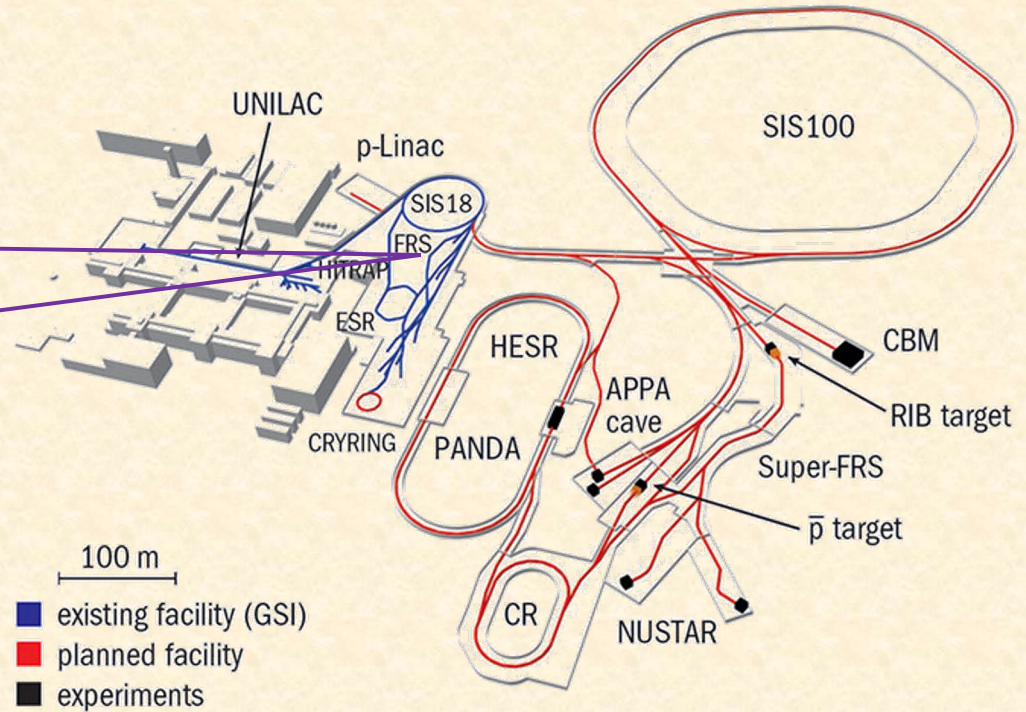
WASA, but upgraded

New superconducting solenoid

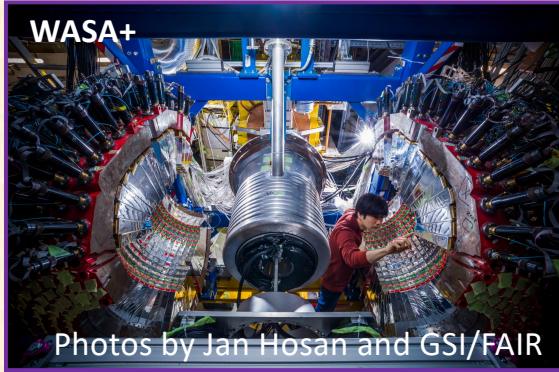
- Electric cooling system
- 2 T
- < 1 M Euro (Toshiba Engineering Co.)

New Inner drift chamber

- Planar type for Forward-detector mode



Our wishes



WASA, but upgraded

New superconducting solenoid

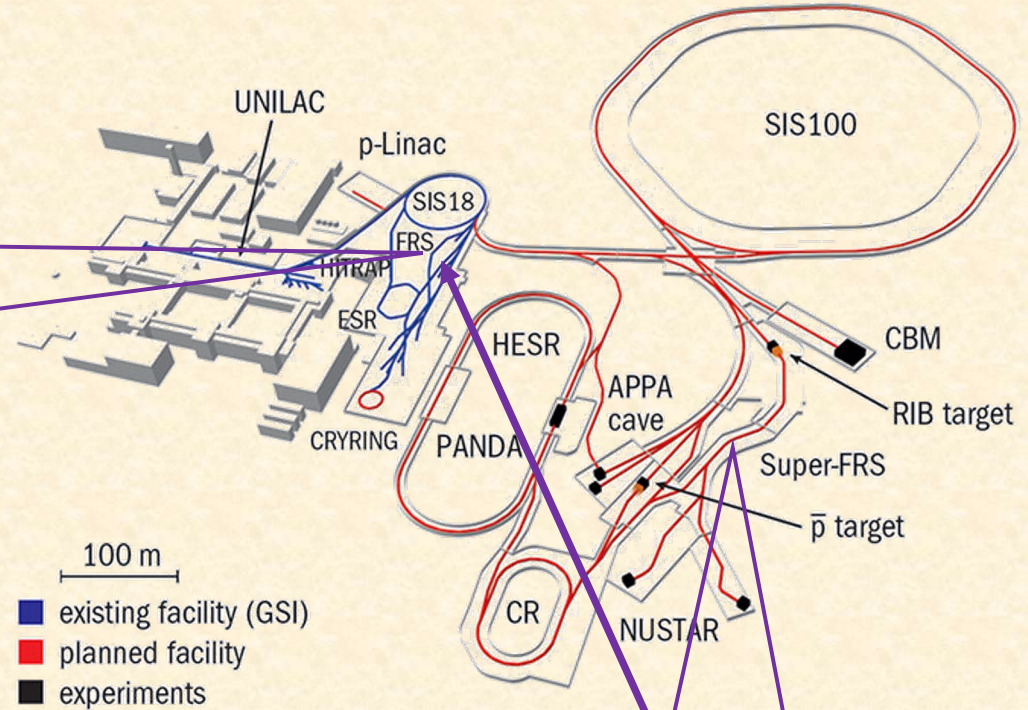
- Electric cooling system
- 2 T
- < 1 M Euro (Toshiba Engineering Co.)

New Inner drift chamber

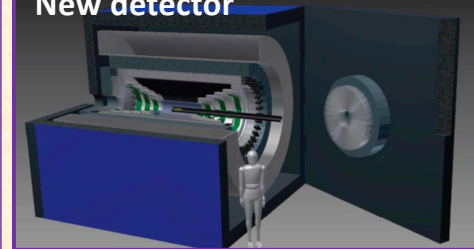
- Planar type for Forward-detector mode

New detector system

- Larger magnet (2m diameter)
- 2 T
- Compact to be installed at the Super-FRS
- Modular detectors (planar and cylindrical)



New detector



Physics subjects

Hypernuclear physics

- Proton rich hypernuclei with proton-rich beams
- Neutron rich hypernuclei with charge-exchange reactions

Mesic-nuclei and –atoms

Baryon resonances in exotic nuclei

Physics subjects

Hypernuclear physics

- Proton rich hypernuclei with proton-rich beams
- Neutron rich hypernuclei with charge-exchange reactions

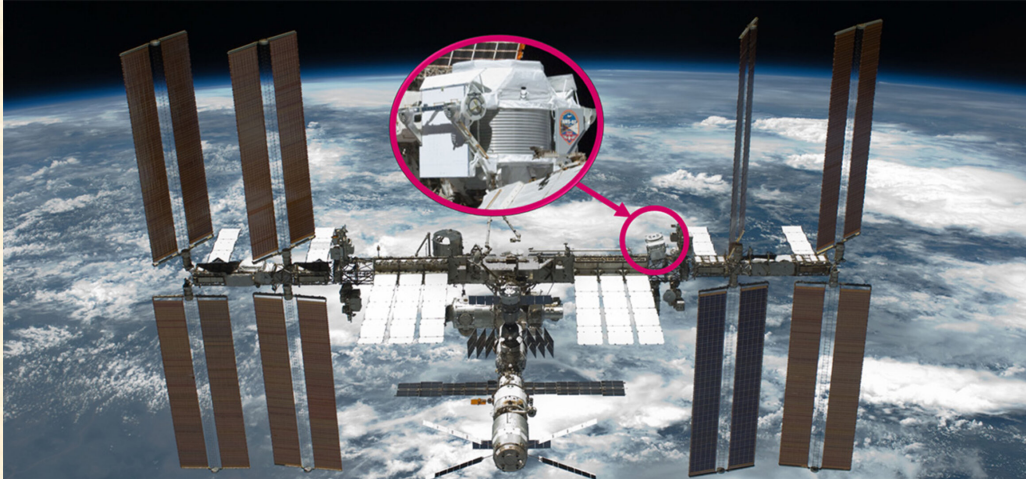
Mesic-nuclei and -atoms

Baryon resonances in exotic nuclei

More physics cases

- Hadron physics with RI-beams
- [Other ideas \(astrophysics, applications, ...\)](#)

AMS-02 in the International Space Station



Search for anti-matter

- Anti-He isotopes

Search for dark-matter candidates

- Annihilation of neutralino

Search for strangelet

Measurements of high energy cosmic rays

Beryllium isotopic composition and Galactic cosmic ray propagation

Paolo Lipari¹, 

¹INFN sezione Roma "Sapienza"

The isotopic composition of beryllium nuclei and its energy dependence encode information of fundamental importance about the propagation of cosmic rays in the Galaxy. The effects of decay on the spectrum of the unstable beryllium-10 isotope can be described introducing the average survival probability $P_{\text{surv}}(E_0)$ that can be inferred from measurements of the isotopic ratio $\text{Be}10/\text{Be}9$ if one has sufficiently good knowledge of the nuclear fragmentation cross sections that determine the isotopic composition of beryllium nuclei at injection. The average survival probability can then be interpreted in terms of propagation parameters, such as the cosmic ray average age, adopting a theoretical framework for Galactic propagation. Recently the AMS02 Collaboration has presented preliminary measurements of the beryllium isotopic composition that extend the observations to a broad energy range ($E_0 \simeq 0.7\text{--}12$ GeV/n) with small errors. In this work we discuss the average survival probability that can be inferred from the preliminary AMS02 data, adopting publically available models of the nuclear fragmentation cross sections, and interpret the results in the framework of a simple diffusion model. This study shows that the effects of decay decrease more slowly than the predictions, resulting in an average cosmic ray age that increases with energy. An alternative possibility is that the cosmic ray age distribution is broader than in the models that are now commonly accepted, suggesting that the Galactic confinement volume has a non trivial structure and is formed by an inner halo contained in an extended one.

I. INTRODUCTION

It is now well established that most of the cosmic rays (CR) observed at the Earth in a broad energy range that extends from $E \sim 10^9$ eV to at least $E \sim 10^{16}$ eV are of Galactic origin, and are generated in the Milky Way, where they remain partially confined by interstellar magnetic fields for a time of order 1–100 Myr. Understanding the properties of CR propagation, and determining the duration and energy (or rigidity) dependence of their Galactic residence time remains a problem of crucial importance for high energy astrophysics.

The study of the flux of the unstable nucleus beryllium-10 (Be10) has been recognised for a long time as a crucially important source of information about the properties of CR propagation. This is because the Be10 decay time ($T_{1/2} \simeq 1.387 \pm 0.012$ Myr) is comparable with the average CR Galactic residence time, and therefore decay can be a significant, or dominant “sink” mechanism in the formation of the spectrum. Comparing the spectral shape of Be10 with those of the stable isotopes Be9 and Be7, allows in principle to measure the effects of decay, and then infer properties of Galactic propagation.

The experimental study of the spectra of individual isotopes, is however a very difficult task, and until now measurements for beryllium have been obtained only at low energy (kinetic energy per nucleon $E_0 \lesssim 2$ GeV) and with rather large errors. Recently, at the 37th International Cosmic Ray Conference in Berlin, the AMS02 Collaboration has presented preliminary measurements of the beryllium isotopes spectra and of the Be10/Be9 ratio with small errors (of order 10–20%), and in a broad energy range ($E_0 \simeq 0.7\text{--}12$ GeV). **These results can be of great value to find answers to some important open questions about CR Galactic propagation.**

In this work, waiting for the publication of the AMS02 observations on the isotopically separated beryllium spectra, we discuss the preliminary results presented at the ICRC, and the best methods to study their astrophysical implications.

*Electronic address: paolo.lipari@roma1.infn.it

Very recent results for $^{10}\text{Be}/^9\text{Be}$ by AMS-02

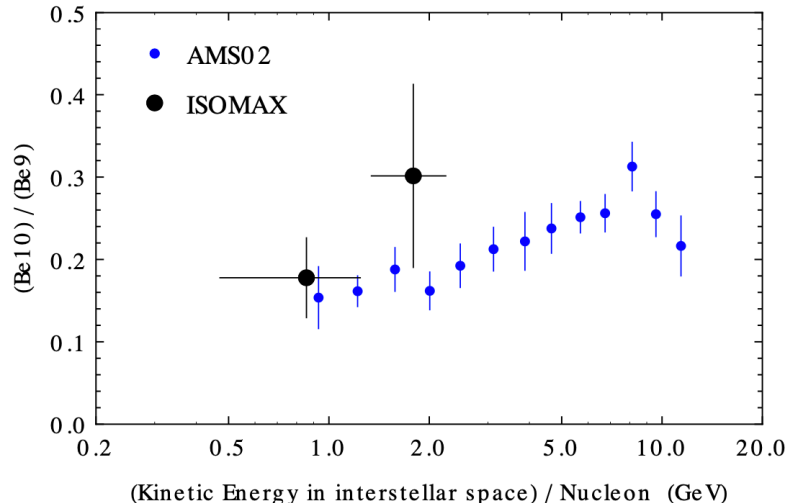


FIG. 1: Measurements of the isotopic ratio beryllium-10/beryllium-9 at high energy, plotted as a function of kinetic energy per nucleon. The data is from ISOMAX [3] and (only preliminary) from AMS02 [2].

What do we want to learn from the $^{10}\text{Be}/^9\text{Be}$?

^9Be : stable

^{10}Be : $T_{1/2} = (1.387 \pm 0.012) \times 10^6$ years

- Similar to a typical period for cosmic rays staying inside the galaxy

$^{10}\text{Be}/^9\text{Be}$ is sensitive to how cosmic rays propagate in the galaxy

- Information on the distribution of the magnetic field (strength and size)
 - It can not be deduced by light since the number of stars in the edge of the galaxy is not sufficient to observe light

What do we want to learn from the $^{10}\text{Be}/^9\text{Be}$?

^9Be : stable

^{10}Be : $T_{1/2} = (1.387 \pm 0.012) \times 10^6$ years

- Similar to a typical period for cosmic rays staying inside the galaxy

$^{10}\text{Be}/^9\text{Be}$ is sensitive to how cosmic rays propagate in the galaxy

- Information on the distribution of the magnetic field (strength and size)
 - It can not be deduced by light since the number of stars in the edge of the galaxy is not sufficient to observe light

Distribution of the magnetic field of the galaxy



Propagation of cosmic-rays



The amount of X-rays induced by reaction of cosmic-rays



If the excess is observed, it can be contributions from dark matter

What do we need to know?

Where are ^9Be and ^{10}Be from?

- Not directly produced by supernova-explosions
- Fragmentation reaction of C/N/O (produced by supernova-explosions) with hydrogen in space

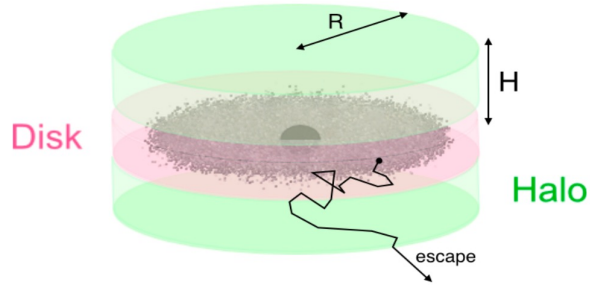


Figure 1. Scheme of the 2D model used for the Galaxy structure. Taken from the lecture <https://w3.ihe.ac.be/~aguilar/PHYS-467/PA3.html>.

	Webber	GALPROP	DRAGON2
D_0 (10^{28} cm 2 s $^{-1}$)	2.3	6.65	7.1
v_A (km/s)	29.9	25.5	27.7
η	-0.25	-0.55	-0.6
δ	0.42	0.44	0.42
H (kpc)	2.07	6.93	6.76

Table 1. Diffusion parameters used in the CR propagation with the different cross section parameterizations. The values have been obtained from the fit of the B/C data from AMS-02 [45, 47] and of the $^{10}\text{Be}/^9\text{Be}$ data from various experiments (see section 8), assuming the different cross section models.

work have shown (see for example Fig. 6) that the same value of P_{surv} can correspond to very different values of the average age of the CR particles in different propagation models. Similarly, a measurement of the energy dependence of the survival probability $P_{\text{surv}}(E_0)$ can be interpreted with different energy dependences of the propagation parameters in different propagation models.

It is easy to see that a survival probability that changes very slowly with energy can be consistent with an average age that is constant or change very slowly with energy if the shape of the age distribution is very broad.

If the CR age distribution is broad, the average survival probability P_{surv} takes (in first approximation) the physical meaning of the fraction of the observed particles with age in the interval $t_{\text{age}} \lesssim T_{\text{dec}}(E_0)$. The decay time grows linearly with the Lorentz factor of the nuclei, and therefore, for a constant shape of the age distribution, P_{surv} increases with energy because the time interval where decay is important becomes smaller. This growth of P_{surv} with energy is slower for a broader distribution.

In the Minimal Diffusion Model the age distribution is determined by two parameters the diffusion times and the halo vertical size. It is however possible for the age distribution to have a more complicated shape that depends on more parameters (that could have different energy dependences). The preliminary AMS02 data (interpreted with current models of the fragmentation cross sections) indicate that when the decay time grows from approximately 4 Myr to approximately 30 Myr the average survival probability remains in rather narrow range ($P_{\text{surv}} \simeq 0.25\text{--}0.4$) suggesting a very broad age distribution where large fractions of particles have ages that are both very short ($t_{\text{age}} \lesssim \text{few Myr}$) and very long ($t_{\text{age}} \gtrsim 50 \text{ few Myr}$). This broad age distribution could exist if the CR confinement volume is formed by an inner halo and a more extended halo (perhaps associated with the existence of the Fermi bubbles) that have confinement times of different orders of magnitude.

The estimate of the CR age distribution is crucially important for the interpretation of the electron and positron spectra, in particular to establish the existence of a new source of relativistic positrons [34–36]. A sufficiently long CR age implies that the large rate of energy losses for e^\mp spectra will result in a strong softening of their spectra, and therefore that the observed hard positron spectrum cannot be generated by the secondary production mechanism and requires a harder source. The preliminary AMS02 beryllium data, as interpreted in the previous section, indicate a CR age that seems to be in conflict with the hypothesis of secondary production for CR positrons. This conclusion is again based on the validity of the current estimates of the nuclear fragmentation cross sections. An approximately constant isotopic ratio for beryllium could in principle be consistent with energy independent fragmentation cross sections and with a short CR age, so that the decay effects for Be10 are small in the entire energy range considered. This interpretation however requires that the observed isotopic composition is equal to the one generated at injection, and this hypothesis is at present strongly disfavoured.

The modeling of nuclear fragmentation cross sections is the main source of systematic uncertainties in extracting the very valuable information encoded in the beryllium isotopic composition. Reducing these uncertainties with an appropriate program of experimental studies is very desirable and of great value.

Acknowledgments

I'm grateful to Pedro De la Torre Luque for help in obtaining the GALPROP nuclear fragmentation cross sections, and to Carmelo Evoli and Michael Korsmeier for interesting discussions.

What do we need to know?

Where are ^9Be and ^{10}Be from?

- Not directly produced by supernova-explosions
- Fragmentation reaction of C/N/O (produced by supernova-explosions) with hydrogen in space

^9Be and ^{10}Be are also fragmented with hydrogen in space during their propagation in the galaxy

Uncertainty is originated from fragmentation reaction cross section

Data of fragmentation reactions are limited, especially at high energies

Fragmentation reaction data

With high energy heavy ion beams with a hydrogen target

- Mainly measured at Bevalac in the Lawrence Berkeley Laboratory (for example, PRC 41 (1990) 547)
- Summarized in PRD 99 (2019) 103023

PHYSICAL REVIEW D 99, 103023 (2019)

Galactic cosmic rays after the AMS-02 observations

Carmelo Evoli¹, Roberto Aloisio, and Pasquale Blasi
¹Gran Sasso Science Institute, Viale F. Crispi 7, 67100 L'Aquila, Italy
and INFN Laboratori Nazionali del Gran Sasso, Via G. Acelli 22, Assergi (AQ), Italy

(Received 24 April 2019; published 28 May 2019)

The unprecedented quality of the data collected by the AMS-02 experiment onboard the International Space Station allowed us to address subtle questions concerning the origin and propagation of cosmic rays. Here we discuss the implications of these data for the injection spectrum of elements with different masses and for the diffusion coefficient probed by cosmic rays through their journey from the sources to the Earth. We find that the best fit to the spectra of primary and secondary nuclei requires (1) a break in the energy dependence of the diffusion coefficient at energies ~ 300 GV; (2) an injection spectrum that is the same for all nuclei heavier than helium, and different injections for both protons and helium. Moreover, if to force the injection spectrum of helium to be the same as for heavier nuclei, the fit to oxygen substantially worsens. Accounting for a small, $X_{\text{He}} \sim 0.4 \text{ g cm}^{-2}$, grammage accumulated inside the sources leads to a somewhat better fit to the B/C ratio but makes the difference between He and other elements even more evident. The statistic and systematic error bars claimed by the AMS collaboration exceed the error that is expected from calculations once the uncertainties in the cross sections of production of secondary nuclei are taken into account. In order to make this point more quantitative, we present a novel parametrization of a large set of cross sections, relevant for cosmic ray physics, and we introduce the uncertainty in the branching ratios in a way that its effect can be easily grasped.

DOI: 10.1103/PhysRevD.99.103023

I. INTRODUCTION

For decades the quest for better data has been constant in the field of cosmic ray (CR) physics. For the first time, at least in the energy region $E \lesssim 1 \text{ TeV}$, the AMS-02 experiment onboard the International Space Station has reversed this situation: statistic and systematic errors on the measured spectra of protons, helium and other primary nuclei, as well as on secondary stable nuclei (boron, lithium, beryllium) are now at the few percent level, thereby providing an unprecedented framework for testing our ideas on the origin and transport of cosmic rays.

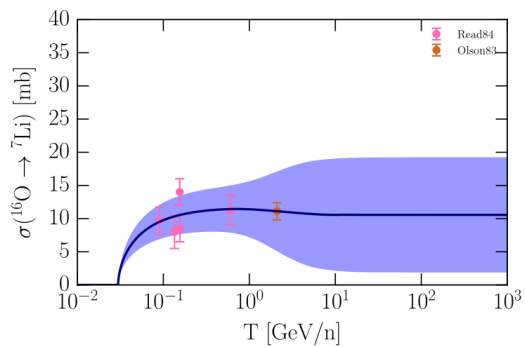
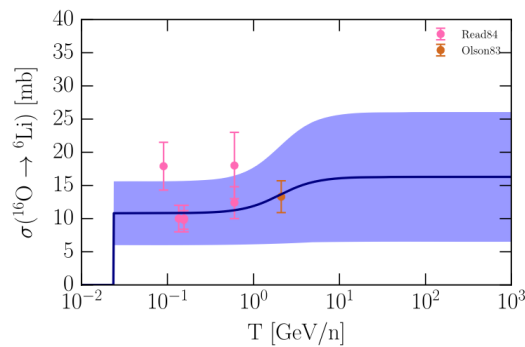
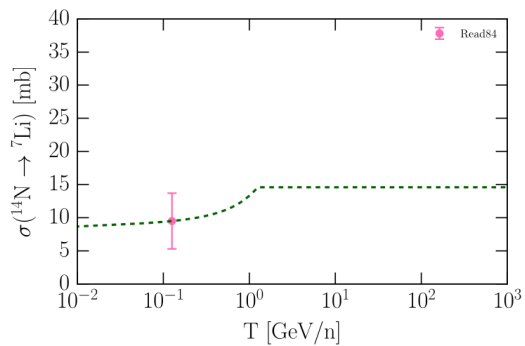
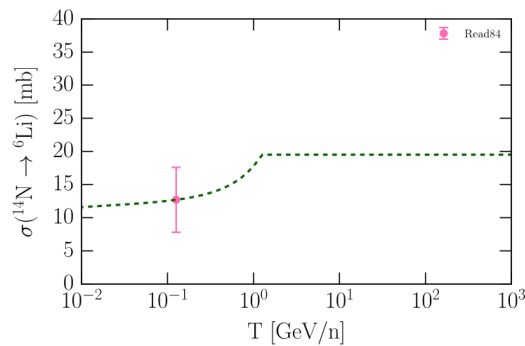
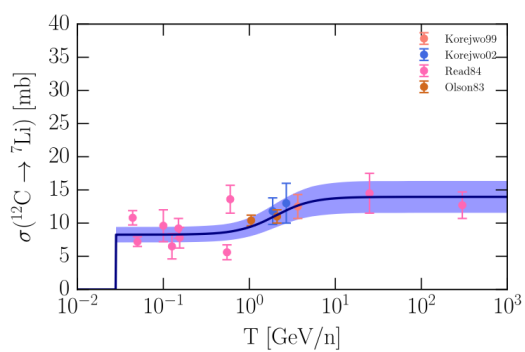
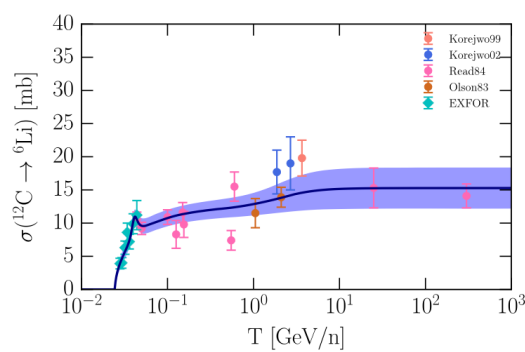
On the other hand, our theoretical ability to make predictions on the spectra of nuclei, especially secondary nuclei, is limited by the uncertainties in the measured values of the cross sections, a point that has been raised by many authors [1–4]. The importance of this point can probably be best illustrated by using the case of boron: the boron-to-carbon ratio is routinely used to infer the mean grammage traversed by CRs while propagating in the Galaxy [5], but the reliability of the grammage depends on the knowledge of boron production cross sections from spallation of heavier elements and on the accuracy of the measurements of the fluxes of such elements (at roughly the same energy per nucleon). Unfortunately the measured

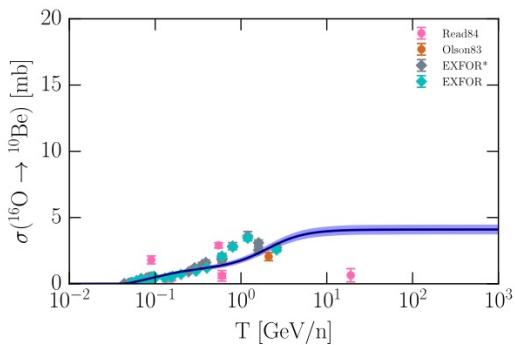
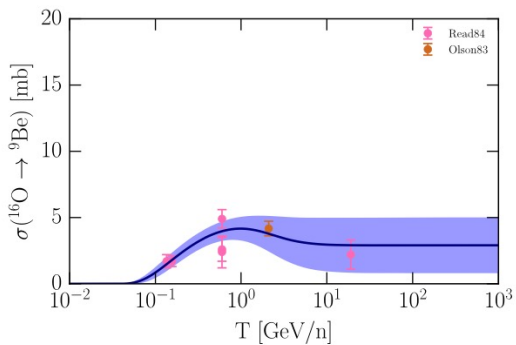
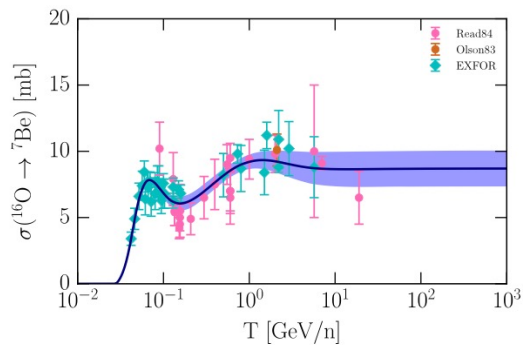
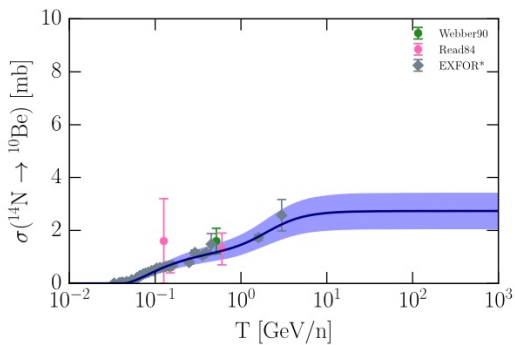
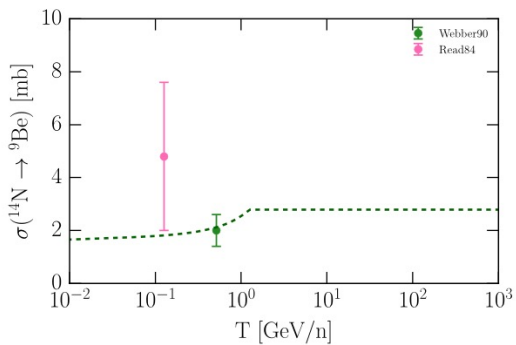
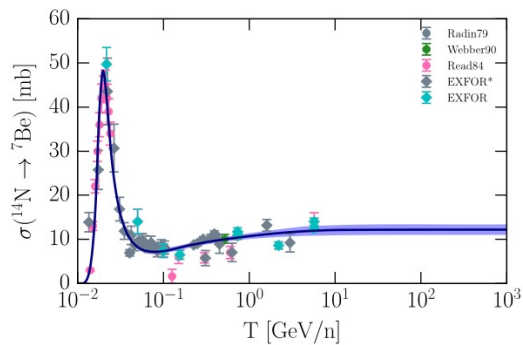
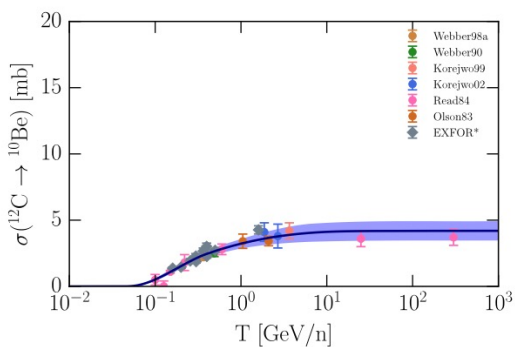
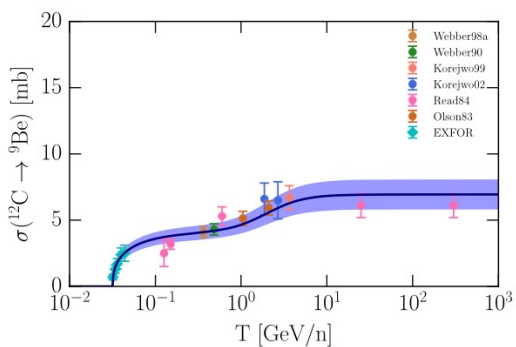
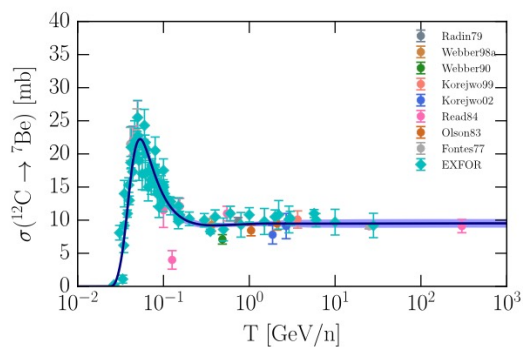
cross sections are known with at least $\sim 30\%$ error (even more for some channels) and the fluxes of elements heavier than carbon, oxygen and nitrogen remain rather uncertain.

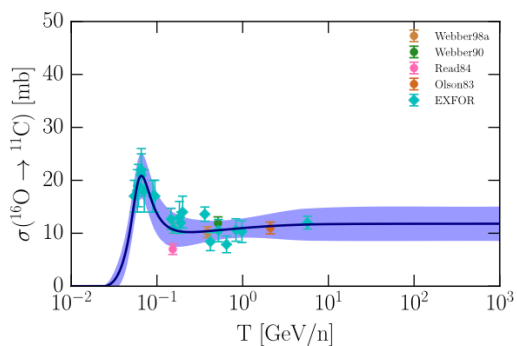
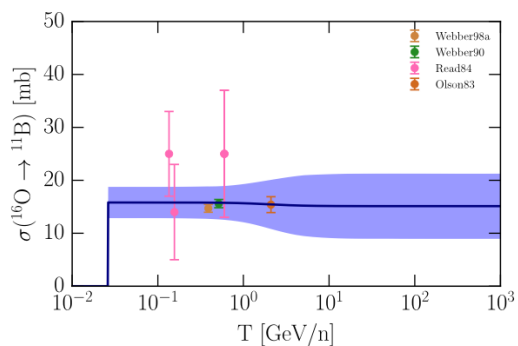
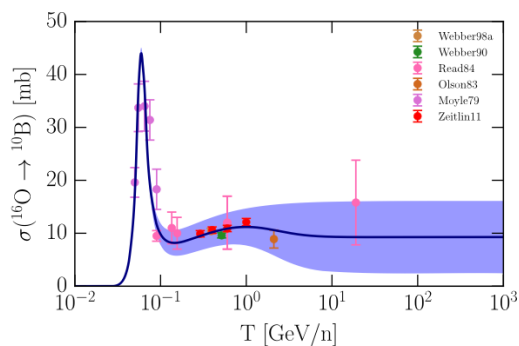
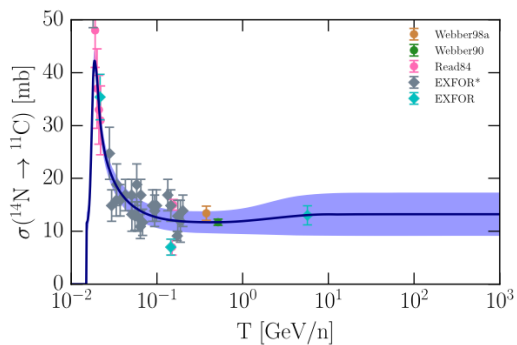
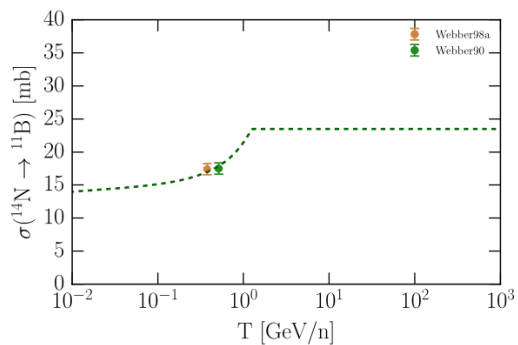
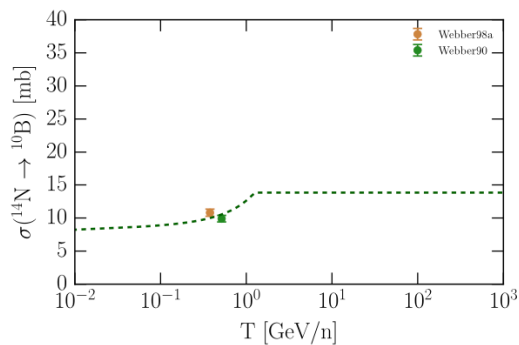
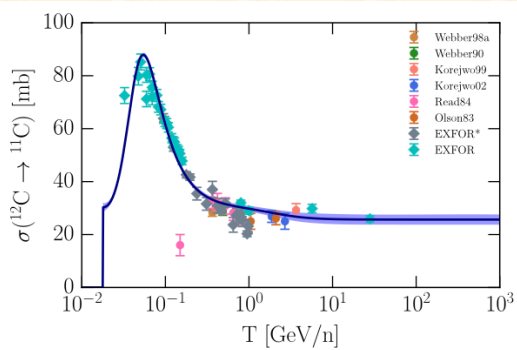
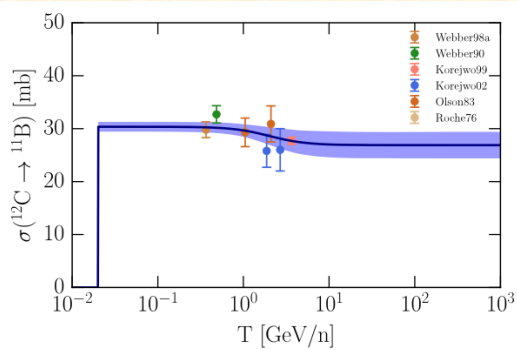
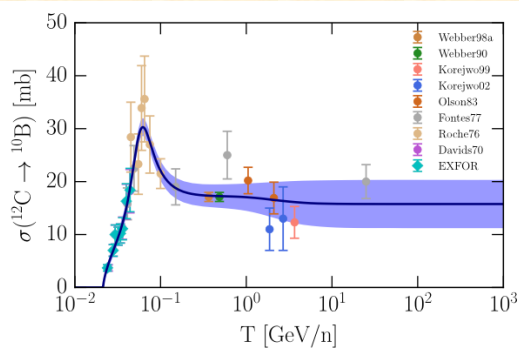
Some major breakthroughs have been made possible by the high precision measurements of AMS-02, first and foremost the detection of breaks in the spectra of virtually all nuclei, most likely hinting at a change of regime in the transport of Galactic CRs at rigidity ~ 300 GV. The anomalous hardening of the spectra of secondary stable nuclei also confirms that most likely the spectral breaks are related to CR transport rather than to subtle aspects of the acceleration process [6]. The rising position ratio [7] and the quasicomponent p/p ratio [8] clearly represent major achievements of this experimental enterprise, with potentially huge implications for our theories on the origin of CRs, to the point that some authors [9, 10] have put forward radically new ideas on the transport of CRs. Testing such ideas is extremely important, but to do so the first step is to understand whether there are serious problems in interpreting data on spectra of primary and secondary nuclei within standard assumptions.

One such assumption, motivated by the fact that most our models for acceleration and transport of CRs are based on a strict rigidity dependence of both processes, is that the source spectra of all nuclei (whatever the sources may be) have the same general shape, especially at energies away from the injection energy and the maximum rigidity [11].

¹carmelo.evoli@gsi.it







^9Be :

- No data at high energies
- Almost no data with ^{14}N beams

^{10}Be

- No data at high energies

Necessity of fragmentation data of
C, N, O \rightarrow ^9Be , ^{10}Be
with a hydrogen target

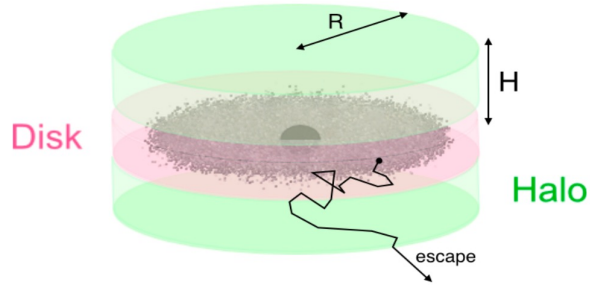


Figure 1. Scheme of the 2D model used for the Galaxy structure. Taken from the lecture <https://w3.ihe.ac.be/~aguilar/PHYS-467/PA3.html>.

	Webber	GALPROP	DRAGON2
D_0 (10^{28} cm 2 s $^{-1}$)	2.3	6.65	7.1
v_A (km/s)	29.9	25.5	27.7
η	-0.25	-0.55	-0.6
δ	0.42	0.44	0.42
H (kpc)	2.07	6.93	6.76

Table 1. Diffusion parameters used in the CR propagation with the different cross section parameterizations. The values have been obtained from the fit of the B/C data from AMS-02 [45, 47] and of the $^{10}\text{Be}/^9\text{Be}$ data from various experiments (see section 8), assuming the different cross section models.

Fragmentation reaction of ${}^9\text{Be}$ and ${}^{10}\text{Be}$

Propagation of ${}^9\text{Be}$ and ${}^{10}\text{Be}$ in the galaxy

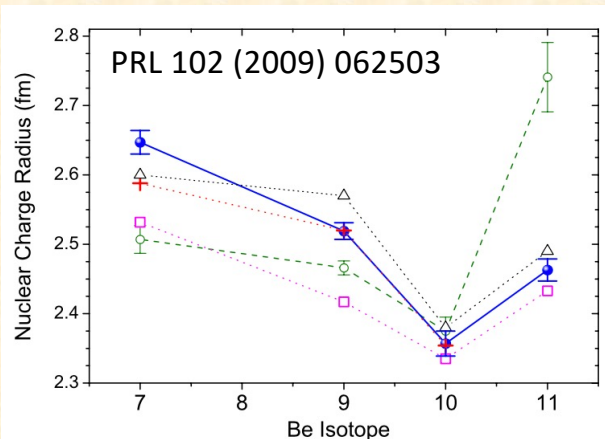
- Assumption: same cross section for ${}^9\text{Be}+p\rightarrow X$ and ${}^{10}\text{Be}+p\rightarrow X$, therefore, no affection on the ${}^{10}\text{Be}/{}^9\text{Be}$ ratio is EXPECTED

Fragmentation reaction of ^9Be and ^{10}Be

Propagation of ^9Be and ^{10}Be in the galaxy

- Assumption: same cross section for $^9\text{Be}+p\rightarrow X$ and $^{10}\text{Be}+p\rightarrow X$, therefore, no affection on the $^{10}\text{Be}/^9\text{Be}$ ratio is EXPECTED

HOWEVER,



Charge radii of ^9Be and ^{10}Be are significantly different

FIG. 3 (color online). Experimental charge radii of beryllium isotopes from isotope-shift measurements (●) compared with values from interaction cross-section measurements (○) and theoretical predictions: Greens-function Monte Carlo calculations (+) [2,24], fermionic molecular dynamics (Δ) [25], *ab initio* no-core shell model (□) [13,26,27].

Fragmentation reaction of ^9Be and ^{10}Be

Propagation of ^9Be and ^{10}Be in the galaxy

- Assumption: same cross section for $^9\text{Be}+p\rightarrow X$ and $^{10}\text{Be}+p\rightarrow X$, therefore, no affection on the $^{10}\text{Be}/^9\text{Be}$ ratio is EXPECTED

HOWEVER,

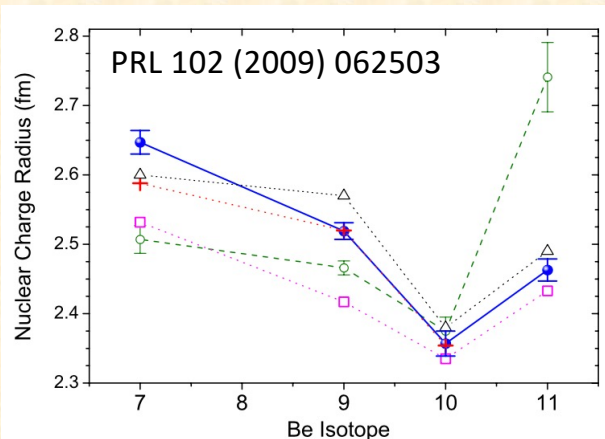


FIG. 3 (color online). Experimental charge radii of beryllium isotopes from isotope-shift measurements (●) compared with values from interaction cross-section measurements (○) and theoretical predictions: Greens-function Monte Carlo calculations (+) [2,24], fermionic molecular dynamics (△) [25], *ab initio* no-core shell model (□) [13,26,27].

Charge radii of ^9Be and ^{10}Be are significantly different

$$^9\text{Be}: (2.519 \text{ fm})^2 = 6.345 \text{ fm}^2$$

$$^{10}\text{Be}: (2.357 \text{ fm})^2 = 5.555 \text{ fm}^2$$

$$5.555/6.345 = 0.875$$

Fragmentation cross section of cosmic ^9Be and ^{10}Be with a hydrogen target must be different

We need precise fragmentation data

Additional interest on the production of ^{10}Be

Low-mass single core-collapse supernova (CCSN) may contribute significantly to understand the the generation/formation of the solar system, and the CCSN could eject more ^{10}Be

- ^{10}Be excess in Calcium-aluminum-rich inclusions in a range of meteoritic samples:

$$^{10}\text{Be}/^9\text{Be} \sim (7.5 \pm 2.5) \times 10^{-4}$$

Additional interest on the production of ^{10}Be

Evidence from stable isotopes and ^{10}Be for solar system formation triggered by a low-mass supernova

Nearly four decades ago Cameron and Truran¹ suggested that the formation of our solar system (SS) might have been due to a single core-collapse supernova (CCSN) whose shock wave triggered the collapse of a nearby interstellar cloud. They recognized that forensic evidence of such an event would be found in CCSN-associated short-lived (≤ 10 Myr) radionuclides (SLRs) that would decay, but leave a record of their existence in isotopic anomalies. Their suggestion was in fact stimulated by observed meteoritic excesses in ^{26}Mg (ref. 2), the daughter of the extinct SLR ^{26}Al with a lifetime of ~ 1 Myr. The inferred value of $^{26}\text{Al}/^{27}\text{Al}$ in the early SS, orders of magnitude higher than the Galactic background, requires a special source.

While simulations support the thesis that a CCSN shock wave can trigger SS formation and inject SLRs into the early SS^{3–6}, detailed modelling of CCSN nucleosynthesis and an accumulation of data on extinct radionuclides have led to a confusing and conflicting picture⁷. CCSNe of ≥ 15 solar masses (M_{\odot}) are a major source of stable isotopes such as ^{24}Mg , ^{28}Si and ^{40}Ca . The contributions from a single CCSN in this mass range combined with the dilution factor indicated by simulations^{4–6} would have caused large shifts in ratios of stable isotopes that are not observed³. A second problem concerns the relative production of key SLRs: such a CCSN source grossly overproduces ^{53}Mn and ^{60}Fe (ref. 3), while producing (relatively) far too little of ^{10}Be . Although the overproduction of ^{53}Mn and ^{60}Fe can plausibly be mitigated by the fallback of core CCSN material, the retention and ejection of these two SLRs^{7,8}, the required fallback must be extremely efficient in high-mass CCSNe.

Here we show that the above difficulties with the CCSN trigger hypothesis can be removed or mitigated, if the CCSN mass was $\lesssim 12 M_{\odot}$. The structure of a low-mass CCSN progenitor differs drastically from that of higher-mass counterparts, being compact with data on binary processes^{9,10}. Given the CCSN trigger hypothesis, we argue that the stable isotopes alone demand such a progenitor. But in addition, this assumption addresses several other problems noted above. First, we show the yields of ^{53}Mn and ^{60}Fe are reduced by an order of magnitude or more in low-mass CCSNe, making the fallback required to bring the yields into agreement with the data much more plausible. Second, we show that the mechanism by which ^{10}Be , the neutron-rich daughter of the two spallation process $^{12}\text{C}(\alpha, n)^{10}\text{Be}$, differs from other SLR production mechanisms in that the yield of ^{10}Be remains high as the progenitor mass is decreased. Consequently we find that an $11.8 M_{\odot}$ model can produce the bulk of the ^{10}Be inventory in the early SS without overproducing other SLRs. We conclude that among possible CCSN triggers, a low-mass one is demanded by the data on binary processes.

It has been commonly thought that ^{10}Be is not associated with stellar sources, originating instead only from spallation of carbon and oxygen in the interstellar medium (ISM) by cosmic rays (CRs)¹¹ or irradiation of the early SS material by solar energetic particles (SEPs)^{10,11} associated with activities of the proto-Sun. It was noted in Yoshida *et al.*¹² that ^{10}Be can be produced by neutrino interactions in CCSNe, but the result was presented for a single model and no connection to meteoritic data was made. Further, to work adopted an old rate for the destruction reaction $^{10}\text{Be}(\alpha, n)^{13}\text{C}$ that is orders of magnitude larger than currently recommended¹³, and therefore, greatly underestimated the ^{10}Be yield.

^{10}Be has been observed in the form of a ^{10}B excess in a range of meteoritic samples. Significant variations across the samples suggest that multiple sources might have contributed to modern CCSN inventory in the early SS^{14–19}. Calcium–aluminum–rich inclusions (CAIs) with $^{26}\text{Al}/^{27}\text{Al}$ close to the canonical value were found to have significantly higher $^{10}\text{Be}/^{9}\text{Be}$ than CAIs with fractionation and unidentified nuclear isotope effects (FUN-CAIs), which also

have $^{26}\text{Al}/^{27}\text{Al}$ much less than the canonical value¹⁸. As FUN-CAIs are thought to have formed earlier than canonical CAIs, it has been suggested²⁰ that the protosolar cloud was irradiated by CRs with a flux $\sim 3 \times 10^4$ times that of FUN-CAIs, by for example, trapping Galactic CRs¹⁸, and that the significantly higher $^{10}\text{Be}/^{9}\text{Be}$ values in canonical CAIs were produced later by SEPs^{10,11}.

A recent study²⁰ showed that trapping Galactic CRs led to little ^{10}Be enrichment of the protosolar cloud and long-term production by Galactic CRs could only provide $^{10}\text{Be}/^{9}\text{Be} \leq 1.3 \times 10^{-4}$. Instead of inferring a large number of CCSNe or a single special CCSN we propose to account for $^{10}\text{Be}/^{9}\text{Be} \sim 3 \times 10^{-4}$. While this pre-enrichment scenario is plausible, it depends on many details of CCSN remnant evolution and CR production and interaction. Similarly, further production of ^{10}Be by SEPs must have occurred at some level, but the actual contributions are sensitive to the composition, spectra and irradiation history of SEPs as well as the composition of the irradiated gas and solids^{10,11,21}, all of which are rather uncertain. In view of both the data and uncertainties in CR and SEP models, we consider it reasonable that a low-mass CCSN provided the bulk of the ^{10}Be inventory in the early SS while still allowing significant contributions from CRs and SEPs. Specifically, we find that such a CCSN can account for $^{10}\text{Be}/^{9}\text{Be} = (7.5 \pm 2.5) \times 10^{-4}$ typical of the canonical CAIs¹⁸. Following the presentation of our detailed model, we discuss a range of alternative sources for ^{10}Be and other SLRs based on our proposed low-mass CCSN trigger and other sources.

Results

Explosion modelling. We have calculated CCSN nucleosynthesis for solar-composition progenitors in the mass range of 11.8 – $30 M_{\odot}$. Each star was evolved to core collapse, using the most recent version of the 1D hydrodynamic code KEPLER^{22–24}. The subsequent explosion was simulated by driving a piston from the base of the oxygen shell into the collapsing progenitor. Piston velocities were selected to produce explosion energies of 0.1, 0.3, 0.6 and $1.2 B$ ($B = 10^{51}$ ergs) for the 11.8 – 12 , 14 , 16 and 18 – $30 M_{\odot}$ models, respectively, to match results from recent CCSN simulations^{25,26}. The material inside the initial radius of the piston was allowed to fall immediately onto the proto-neutron star forming at the core. In our initial calculations, shown in Fig. 1 and labelled Case 1 in Table 1, we assume all material outside the piston is ejected. Neutrino emission was modelled by assuming Fermi–Dirac spectra with chemical potentials $\mu = 0$, fixed temperatures $T_{\nu} \sim 3$ MeV and $T_{\bar{\nu}} \sim T_{\nu} \sim T_{\nu} \sim T_{\bar{\nu}} \sim 5$ MeV, and luminosities decreasing exponentially from an initial value of $1.67 B s^{-1}$ per species, governed by a time constant of ~ 3 s. This treatment is consistent with detailed neutrino transport calculations²⁷ as well as supernova 1987A observations²⁸. A full reaction network was used to track changes in composition during the evolution and explosion of each star, including neutrino rates taken from Heger *et al.*²⁹

Nucleosynthesis yields. Figure 1 shows the yields normalized to the $11.8 M_{\odot}$ model as functions of the progenitor mass for stable isotopes ^{12}C , ^{16}O , ^{24}Mg , ^{28}Si , ^{40}Ca and ^{56}Fe as well as SLRs ^{10}Be , ^{41}Ca , ^{53}Mn , ^{60}Fe and ^{107}Pd . It can be seen that except for ^{10}Be , the yields of all other isotopes increase sharply for CCSNe of 14 – $30 M_{\odot}$. Therefore, a high-mass CCSN trigger is problematic, generating unacceptably large shifts in ratios of stable isotopes and overproducing SLRs such as ^{53}Mn and ^{60}Fe (ref. 3). Fallback of $\geq 1 M_{\odot}$ of inner material in such CCSNe was invoked in Takigawa *et al.*⁸ to account for the data on the SLRs ^{26}Al , ^{41}Ca , ^{53}Mn and ^{60}Fe . Using our models (Supplementary Table 1), we

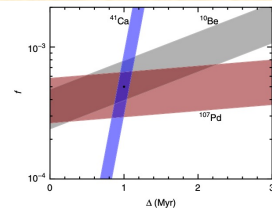


Figure 2 | Relations between parameters characterizing the core-collapse supernova trigger. The parameter f denotes the fraction of the yields of short-lived radionuclides incorporated into the proto-solar cloud, per solar mass. The parameter Δ denotes the time between the supernova explosion and incorporation of short-lived radionuclides into early solar system solids. Results are calculated from equation (1) using yields for the 11.8 – 30 -solar-mass model with no fallback (Case 1) and meteoritic data for ^{10}Be , ^{41}Ca and ^{107}Pd with 2σ uncertainties (Table 1). The filled circle at $f = 5 \times 10^{-5}$ and $\Delta \sim 1$ Myr is the approximate best-fit point within the overlap region.

updated estimates with uncertainties⁴⁶). The yield obtained with the laboratory rate accounts for almost all of the ^{182}Hf in the early SS. This removes a conflict with data on the SLR ^{129}I that arises when ^{182}Hf is attributed to the rapid neutron-capture (r) process^{46,48}.

Role of fallback. The Case 1 results of Table 1 are consistent with the meteoritic data on ^{26}Al , ^{36}Cl , ^{135}Cs , ^{182}Hf and ^{209}Po , as the contributions do not exceed the measured values. In contrast, although the production of ^{53}Mn and ^{60}Fe is greatly reduced in low-mass CCSNe, the ^{53}Mn contribution remains a factor of 60 too large, while ^{60}Fe is compatible only with the larger of the two observed values (Table 1). Both of these SLRs originate from zones deep within the $11.8 M_{\odot}$ star: ^{53}Mn is produced in the innermost 10 – $2 M_{\odot}$ of the shocked material, while $\sim 90\%$ of the ^{60}Fe is associated with the innermost $0.12 M_{\odot}$. Because of the low explosion energy used here based on simulations²⁶, the expected fallback of the innermost shocked zones onto the proto-neutron star²⁹ provides a natural explanation for the discrepancies: most of the produced ^{53}Mn and, possibly, ^{60}Fe is not ejected. In Case 2 of Table 1, where only 1.5% of the innermost $1.02 \times 10^{-2} M_{\odot}$ is ejected, $^{53}\text{Mn}/^{55}\text{Mn}$ is reduced to its measured value $(6.28 \pm 0.66) \times 10^{-6}$ (ref. 38), while other SLR contributions are largely unaffected. In Case 3, where only 1.5% of the innermost $0.116 M_{\odot}$ is ejected, additional large reductions (a factor of ~ 10) are found for ^{60}Fe and ^{182}Hf , accompanied by smaller decreases (a factor of ~ 2) in ^{26}Al , ^{36}Cl , ^{135}Cs and ^{209}Po .

Case 3 represents the limit of reducing ^{53}Mn and ^{60}Fe without affecting the concordance among ^{10}Be , ^{41}Ca and ^{107}Pd (Supplementary Fig. 1; Supplementary Discussion). Were the lower observed value for ^{60}Fe (ref. 39) proven correct, we would have to either reduce its yield by examining the significant nuclear and stellar physics uncertainties^{49,50} or use even more substantial fallback to reconsider the low-mass CCSN contributions to SLRs. Because of the correlated effects of fallback on ^{60}Fe and ^{182}Hf , more fallback would also rule out an attractive explanation for the latter, as described above. Note that the fallback assumed for Cases 2 and 3 is far below that

invoked for high-mass CCSNe in Takigawa *et al.*⁸ to account for ^{26}Al , ^{41}Ca , ^{53}Mn and the higher observed value of ^{60}Fe .

If, however, the higher ^{60}Fe value⁴⁹ is correct, then a plausible scenario like Case 2, where SS formation was triggered by a low-mass CCSN with modest fallback, would be in reasonably agreement with the data on ^{10}Be , ^{41}Ca , ^{53}Mn , ^{60}Fe and ^{107}Pd . The nuclear fission, notably the rapidly decaying ^{41}Ca , determines the delay between the CCSN explosion and incorporation of SLRs into early SS solids, $\Delta \sim 1$ Myr. The deduced fraction of CCSN material injected into the protosolar cloud, $f = 5 \times 10^{-5}$, is consistent with estimates based on simulations of ejecta interacting with dense gas⁵¹ and is in reasonable agreement (Discussion). There is also an implicit connection to the CCSN explosion energy, which influences fallback in hydrodynamic models.

Discussion

In addition to neutrino-induced production, a low-mass CCSN can make ^{10}Be through CRs associated with its remnant evolution²⁰. However, the yield of this second source is modest (Supplementary Discussion). The net yield in the ISM trapped within the remnant is limited by the amount of this ISM. Production within the general protosolar cloud during its initial contact with the remnant (that is, before thorough mixing of the injected material) would also be expected, and the yield could possibly account for $^{10}\text{Be}/^{9}\text{Be} \sim 3 \times 10^{-4}$ in FUN-CAIs¹⁸. However, FUN-CAIs are rare, and their ^{10}Be inventory may be more consistent with local production by the CCSN Crs. Taking the net CR contribution averaged over the protosolar cloud to be $^{10}\text{Be}/^{9}\text{Be} \sim 10^{-4}$, a value that we argue is more consistent with long-term production by Galactic CRs¹⁸, we add the neutrino-produced $^{10}\text{Be}/^{9}\text{Be} = (5.2 \pm 6.4) \times 10^{-4}$ (Table 1) from the CCSN to obtain $^{10}\text{Be}/^{9}\text{Be} = (6.2 \pm 7.4) \times 10^{-4}$, which is in accord with $^{10}\text{Be}/^{9}\text{Be} = (7.5 \pm 2.5) \times 10^{-4}$ observed in canonical CAIs. In general, we consider that neutrino-induced production provided the baseline ^{10}Be inventory in these samples and the observed variations^{14,16,18,19} can be largely attributed to local production by SEPs.

Our proposal that a low-mass CCSN trigger provided the bulk of the ^{10}Be inventory in the early SS has several important features: (1) the relevant neutrino and CCSN physics is known reasonably well, and the uncertainty in the ^{10}Be yield is estimated here to be within a factor of ~ 2 ; (2) the production of both ^{10}Be and ^{41}Ca is in agreement with observations^{36,37}, a result difficult to achieve by SEPs¹⁵; and (3) the yield pattern of ^{10}Be and ^{41}Ca isotopes (Supplementary Table 4) is distinctive, with predominant production of ^{11}B and ^{11}B and differing greatly from patterns of production by CRs and SEPs, so that precise meteoritic data might provide distinguishing tests (Supplementary Discussion).

We emphasize that while ^{53}Mn and ^{60}Fe production is greatly reduced in a low-mass CCSN, some fallback is still required to explain the meteoritic data. The fallback solution works well for ^{53}Mn (Table 1). When somewhat different meteoritic values of $^{53}\text{Mn}/^{55}\text{Mn}$ (refs 52,53) are used, only the ejected fractions of the innermost shocked material need to be adjusted accordingly. The case of ^{60}Fe is more complicated. The meteoritic measurements are difficult, especially in view of a recent study showing the mobility of ^{60}Fe and Ni in the relevant samples⁵⁴. Another recent study gave meteoritic values of $^{60}\text{Fe}/^{56}\text{Fe} = 2.6 \times 10^{-7}$ (ref. 55), which may be accounted for by Case 3 of our model (Table 1). However, were $^{60}\text{Fe}/^{56}\text{Fe} = 10^{-8}$ (ref. 39), currently preferred by many workers, to be confirmed, we would have to conclude that either the present ^{60}Fe yield of the low-mass CCSN is wrong or its contributions to SLRs must be reconsidered.

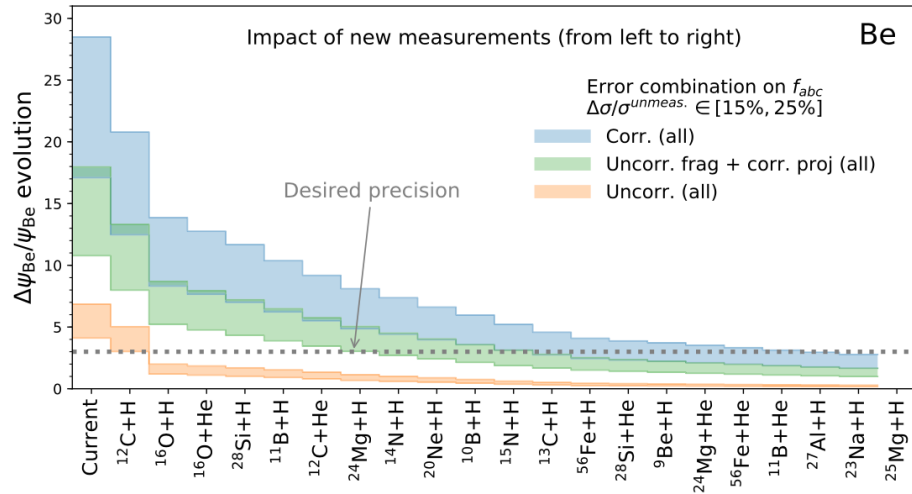
Production of ^{10}Be

- Precise measurement of ^9Be and ^{10}Be fragmentation reaction cross section
- Theoretical calculations including the propagation of ^9Be and ^{10}Be
- Deducing the contribution on the amount of ^{10}Be by the Low-mass single core-collapse supernova (CCSN)
- Contributing to understand the generation/formation of the solar system

Importance of the precision

Not only for C/N/O/Be+p, but also the others

PHYSICAL REVIEW C 98, 034611 (2018)



Current precision for the amount of Be: about 28%

To improve down to 10 %

- $^{12}\text{C} + \text{H}$
- $^{16}\text{O} + \text{H}$
- $^{16}\text{O} + \text{He}$
- $^{28}\text{Si} + \text{H}$
- $^{11}\text{B} + \text{H}$
- $^{12}\text{C} + \text{He}$
- $^{24}\text{Mg} + \text{H}$
- $^{14}\text{N} + \text{H}$

We need various fragmentation cross section data at high energies

Contribution from heavier nuclei

Astronomy & Astrophysics manuscript no. libeb_update
September 1, 2022

©ESO 2022

Ne, Mg, Si, Fe \rightarrow Li, Be, B

- 20 % contribution
- Almost NO DATA

The importance of Fe fragmentation for LiBeB analyses

Is a Li primary source needed to explain AMS-02 data?

D. Maurin¹*, E. Ferronato Bueno^{2**}, Y. Génolini^{3,4***}, L. Derome¹, and M. Vecchi²

¹ LPSC, Université Grenoble Alpes, CNRS/IN2P3, 53 avenue des Martyrs, 38026 Grenoble, France

² Kapteyn Astronomical Institute, University of Groningen, Landleven 12, 9747 AD Groningen, The Netherlands

³ LAPTh, Université Savoie Mont Blanc & CNRS, Chemin de Bellevue, 74941 Annecy Cedex, France

⁴ Niels Bohr International Academy & Discovery Center, Niels Bohr Institute, University of Copenhagen, Blegdamsvej 17, DK-2100 Copenhagen, Denmark

Received / Accepted

ABSTRACT

Context. High-precision data from AMS-02 on Li, Be, and B provide the best constraints on Galactic cosmic-ray transport parameters. **Aims.** We re-evaluate the impact of Fe fragmentation on the Li, Be, and B modelling. We discuss the consequences on the transport parameter determination and reassess whether a primary source of Li is needed to match AMS-02 data.

Methods. We renormalised several cross-section parametrisations to existing data for the most important reactions producing Li, Be, and B. We used the usmc code with these new cross-section sets to re-analyse Li/C, Be/C, and B/C AMS-02 data.

Results. We built three equally plausible cross-section sets. Compared to the initial cross-section sets, they lead to an average enhanced production of Li (~ 20 – 50%) and Be (~ 5 – 15%), while leaving the B flux mostly unchanged. In particular, Fe fragmentation is found to contribute to up to 10% of the Li and Be fluxes. Used in the combined analysis of AMS-02 Li/C, Be/C, and B/C data, the fit is significantly improved, with an enhanced diffusion coefficient ($\sim 20\%$). The three updated cross-section sets are found to either slightly underfoot or overfoot the Li/C and B/C ratios; this strongly disfavors evidence for a primary source of Li in cosmic rays. We stress that isotopic cosmic-ray ratios of Li (and to a lesser extent Be), soon to be released by AMS-02, are also impacted by the use of these updated sets.

Conclusions. Almost no nuclear data exist for the production of Li and B isotopes from Ne, Mg, Si, and Fe, whereas these reactions are estimated to account for $\sim 20\%$ of the total production. New nuclear measurements would be appreciated and help to better exploit the high-precision AMS-02 cosmic-ray data.

Key words. Astroparticle physics – Cosmic rays – Diffusion – Nuclear reactions

arXiv:2203.00522v2 [astro-ph.HE] 31 Aug 2022

1. Introduction

Galactic cosmic-ray (GCR) Li, Be, and B (hereafter LiBeB for short) isotopes are present in minute amount in the Solar System, but are seen in excess in cosmic-ray (CR) data (e.g. Tatischeff & Gabici 2018). These CR species are denoted secondary species, as they are generally assumed to be produced only by a nuclear interaction of heavier CR species on the interstellar medium (ISM). The dominant channels for this production are the direct production of LiBeB from C and O CR fluxes (e.g. Génolini et al. 2018). The latter fluxes are among the most abundant CR species, and are of primary origin, that is they result almost solely from the diffusive shock wave acceleration of the ISM material. The study of secondary species, or secondary-to-primary ratios, plays a central role in CR physics because they calibrate the transport parameters in the Galaxy. The latter can give insight into the micro-physics of transport in the turbulent medium (e.g. Génolini et al. 2019), but it is also a central ingredient for many related studies (e.g. electron and positron spectra, γ -ray diffuse emissions, indirect searches for dark matter in CRs).

The AMS-02 experiment on-board the International Space Station has collected an unprecedented number of CRs (Aguilar et al. 2021a); the data published by the collaboration reach the few percent level of precision. The LiBeB data, which display a spectral break at ~ 200 GV (Aguilar et al. 2018a), have been used by several authors to study the transport of GCRs (Génolini et al. 2017, 2019; Evoli et al. 2019; Weirich et al. 2020b; Bouchini et al. 2020a,b; Yuan et al. 2020; De La Torre Lique et al. 2021a). The above studies assume no extra source of LiBeB, but it remains possible to have a small amount of secondary production inside the acceleration site (Mertsch et al. 2021; Kawakana & Lee 2021), or even to have a primary source of Li (Kawakana & Yanagita 2018) from nova explosions (Hernanz 2015).

All model calculations rely on a network of CR fragmentation reactions. Uncertainties on these reactions range from 10% to 20%, and are a limiting factor to take full advantage of the high-precision CR data (Génolini et al. 2018). For this reason, possible excesses or mismatches (between the model and the data) must be robustly checked against nuclear uncertainties (among others). A new methodology to account for and propagate these uncertainties was proposed in Derome et al. (2019). The main idea was to start from a given production nuclear dataset and, while fitting LiBeB data, to allow the most relevant reactions to vary around their central values; penalties prevent cross sections from wandering far away from their expected

* david.maurin@lpsc.in2p3.fr
** e.ferronato.bueno@rug.nl
*** yoann.genolini@lapth.cnrs.fr

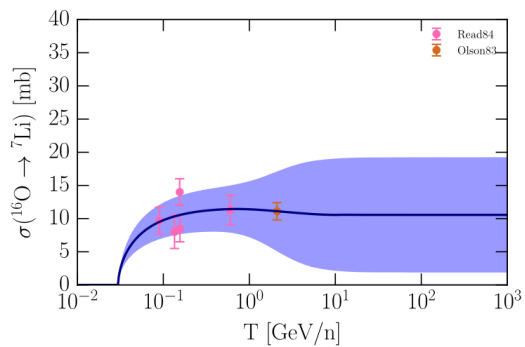
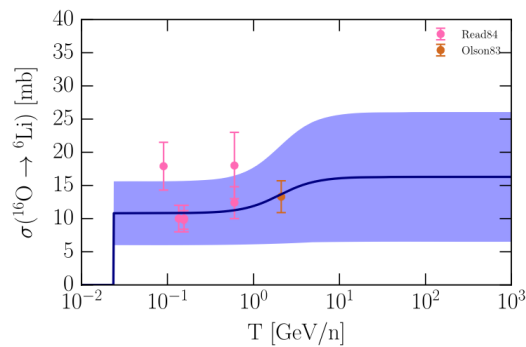
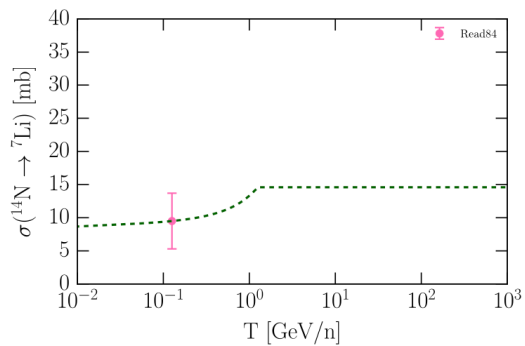
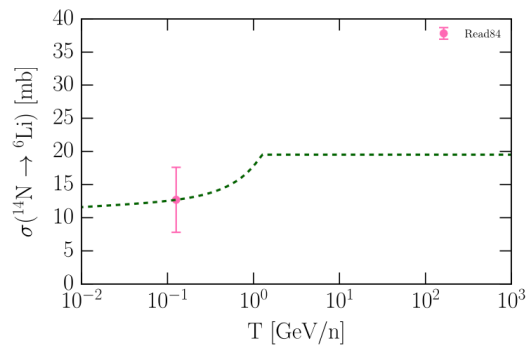
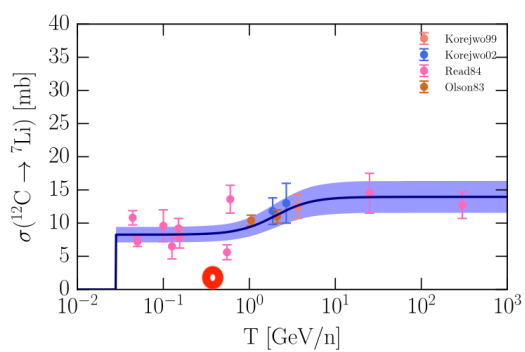
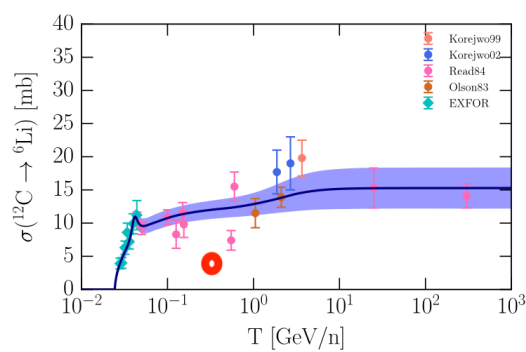
Unpublished Fragmentation cross section data

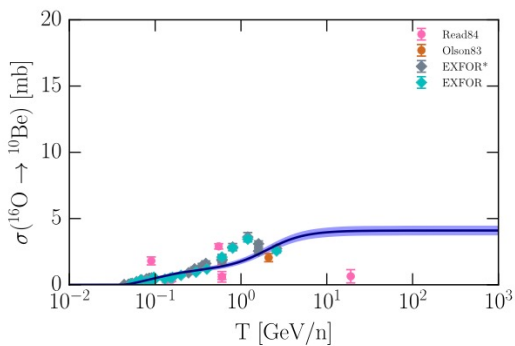
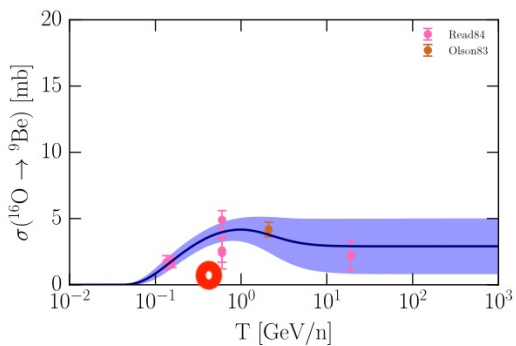
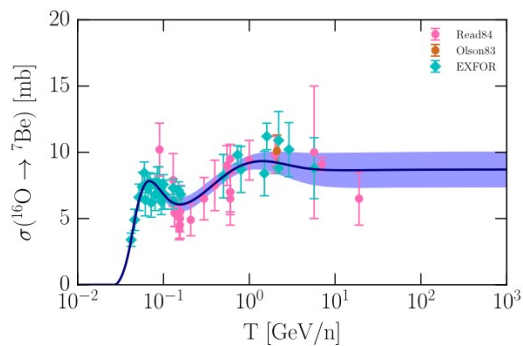
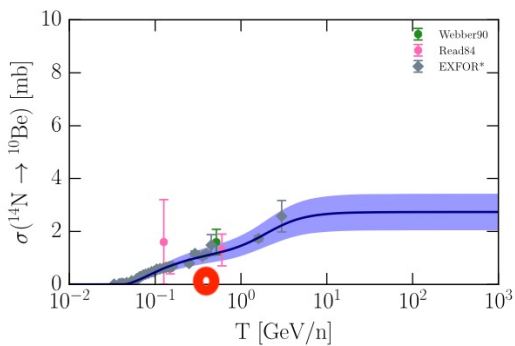
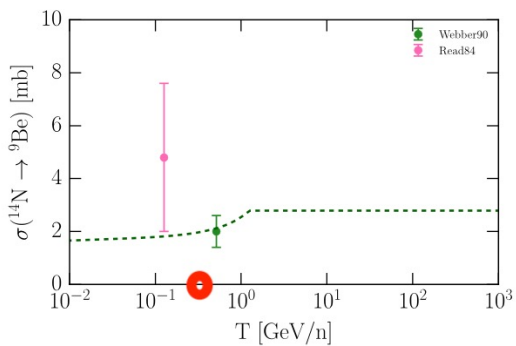
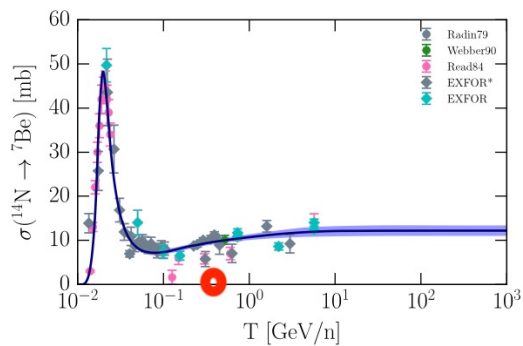
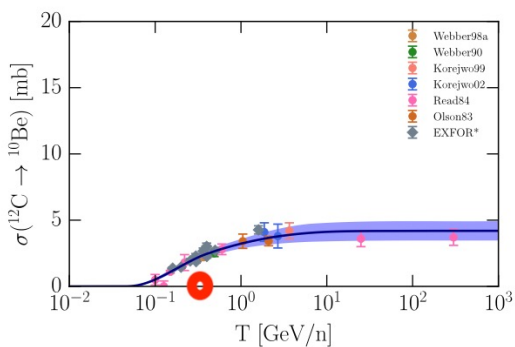
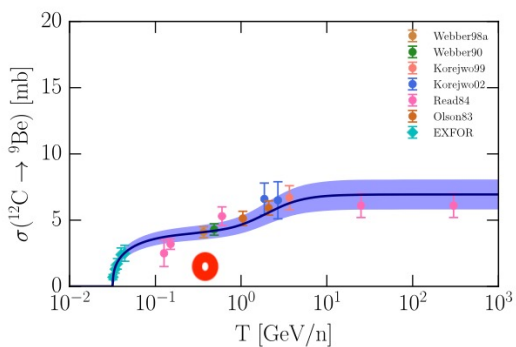
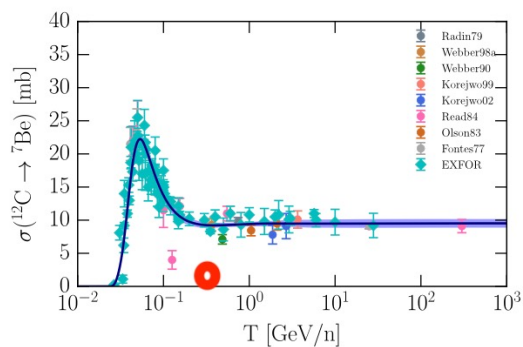
Private communication

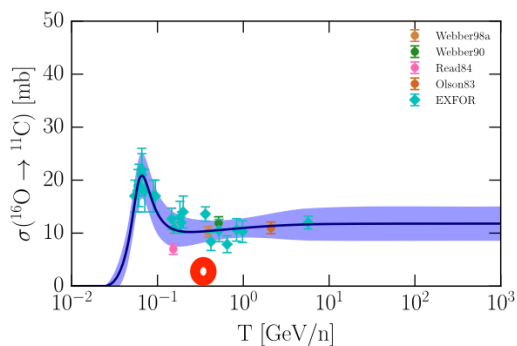
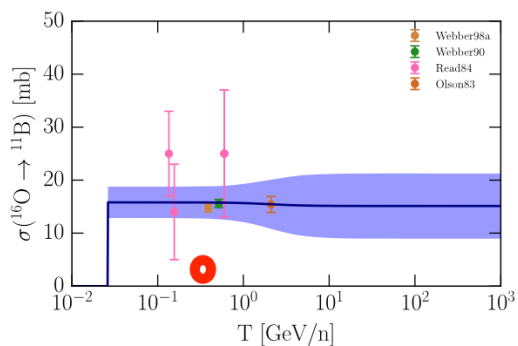
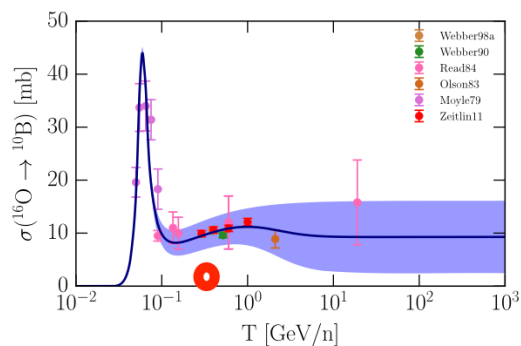
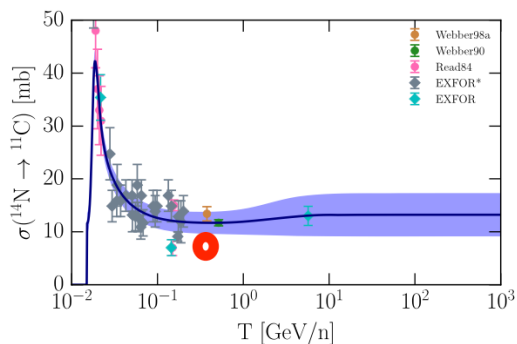
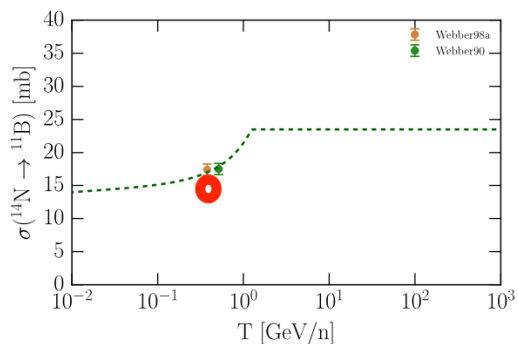
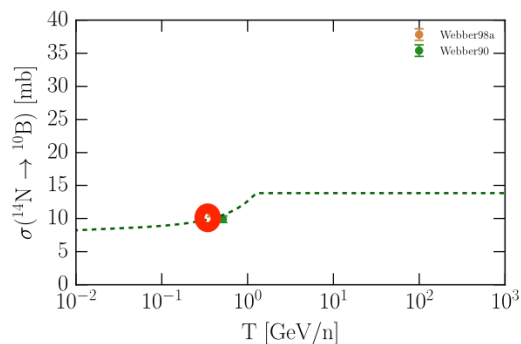
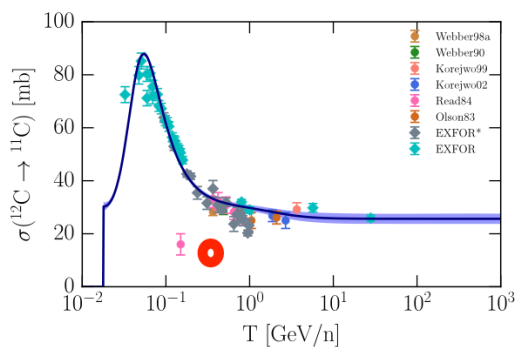
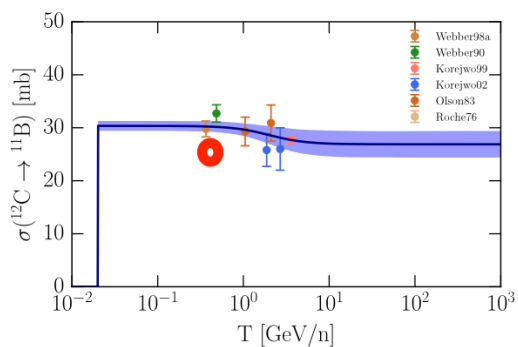
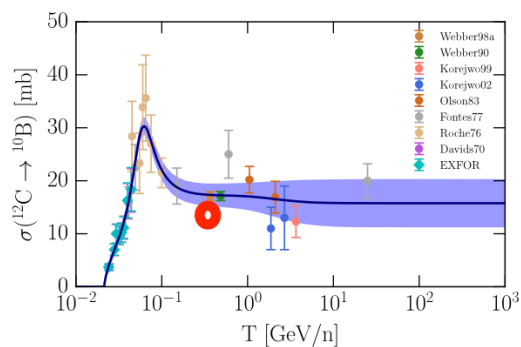
- Proton target
- 308 – 450 A MeV
- ^{12}C , ^{14}N and $^{13,14,15,16,20,22}\text{O}$ projectiles

TABLE I. Summary of the fragmentation cross sections (with statistics and systematic uncertainties) studied in this work for different projectiles, $^{13,14,15,16,20,22}\text{O}$, ^{14}N and ^{12}C , impinging on a proton target. Each reaction channel is characterized by the (Z,A) numbers for projectiles (subscript p) and outgoing fragments (f), and the projectile energies at half fragmentation target.

$E(\text{A MeV})$	$(Z,A)_p$	$(Z,A)_f$	$\sigma_{frag}(\text{mb})$	$E(\text{A MeV})$	$(Z,A)_p$	$(Z,A)_f$	$\sigma_{frag}(\text{mb})$	$E(\text{A MeV})$	$(Z,A)_p$	$(Z,A)_f$	$\sigma_{frag}(\text{mb})$
397	8,13	7,12	415	8,20	8,19	8,19	450	6,12	6,11	6,11	4,10
		6,12				8,18				6,10	
		6,11				8,17				5,11	
		6,10				8,16				5,10	
		6,9				8,15				5,8	
		5,11				7,19				4,10	
		5,10				7,18				4,9	
		5,8				7,17				4,7	
		4,9				7,16				3,8	
		4,7				7,15				3,7	
						7,14				3,6	
						6,17					
		349				8,14				8,13	
7,13	8,21		7,12								
7,12	8,20		6,14								
7,11	8,19		6,13								
6,12	8,18		6,12								
6,11	8,17		6,11								
6,10	8,16		6,10								
6,9	8,15		5,12								
5,11	7,21		5,11								
5,10	7,20		5,10								
5,8	7,19		5,8								
4,10	7,18		4,11								
4,9	7,17		4,10								
4,7	7,16	4,9									
308	8,15	8,14	414	8,22	8,21	450	7,14	7,13	7,13	4,10	
		8,13			8,20				7,12		
		7,14			8,19				6,14		
		7,13			8,18				6,13		
		7,12			8,17				6,12		
		6,13			8,16				6,11		
		6,12			8,15				5,15		
		6,11			7,21				5,14		
		6,10			7,20				5,13		
		6,9			7,19				5,12		
		5,11			7,18				5,11		
		5,10			7,17				5,10		
		4,10			7,16				4,11		
4,9	7,15	4,10									
4,7	7,14	4,9									
450	8,16	8,15	414	8,22	6,17	450	7,14	7,13	7,13	4,10	
		8,14			8,21				6,16		
		7,15			8,20				6,15		
		7,14			8,19				6,14		
		7,13			8,18				6,13		
		7,12			8,17				6,12		
		6,14			8,16				6,11		
		6,13			8,15				5,15		
		6,12			7,21				5,14		
		6,11			7,20				5,13		
		6,10			7,19				5,12		
		5,13			7,18				5,11		
		5,12			7,17				5,10		
5,11	7,16	4,11									
5,10	7,15	4,10									
4,10	7,14	4,9									
4,9	7,13	4,7									







What do we want to achieve?

Precise measurement of fragmentation reactions at high energies

- With stable heavy ion beams: Be, B, C, N, O, Mg and Si on H/He target
- RI-beams: especially ^{10}Be on H target
- We have to identify final channels (isotopes clearly)
 - Possible only with FRS/Super-FRS at GSI/FAIR
 - Using the setup at the CBM cave (10 A GeV) is not practical to provide clear isotope identifications

However, we can currently only up to around 2 A GeV with FRS/Super-FRS

We need a robust cross section model up to 10 A GeV

Exclusive measurement including all final states by measuring nuclei, baryons and mesons up to at 2 A GeV



Constructing a robust fragmentation reaction model, also valid at 10 A GeV



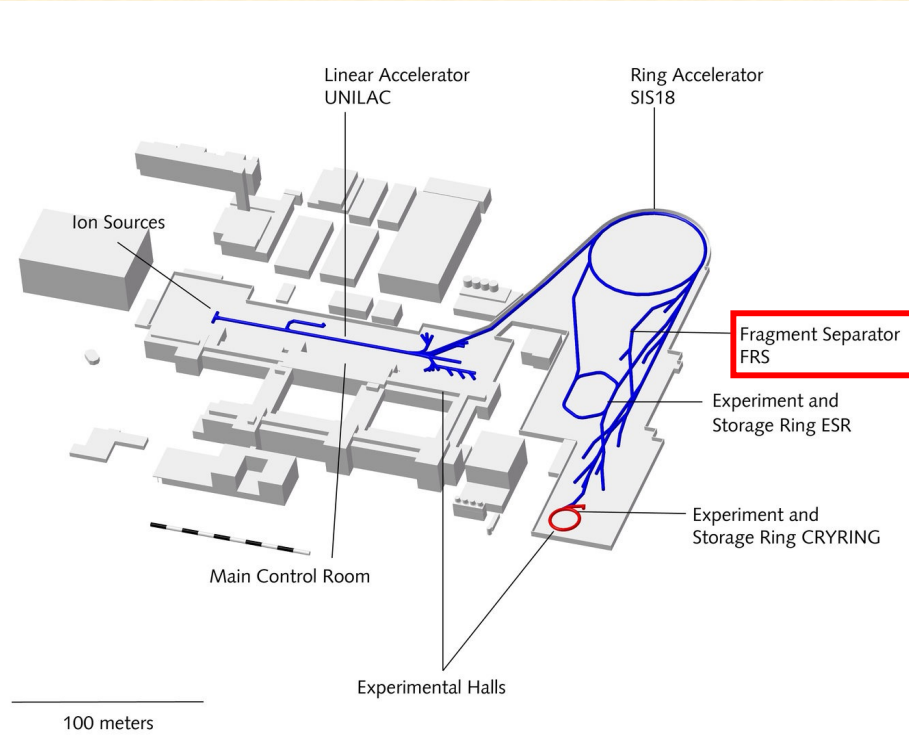
Validating the model to measure inclusive fragment cross sections at 10 A GeV at the CBM cave



By using the constructed fragmentation model, one can perform theoretical calculations for the propagation of cosmic-rays, thus then reveal the structure of the galaxy

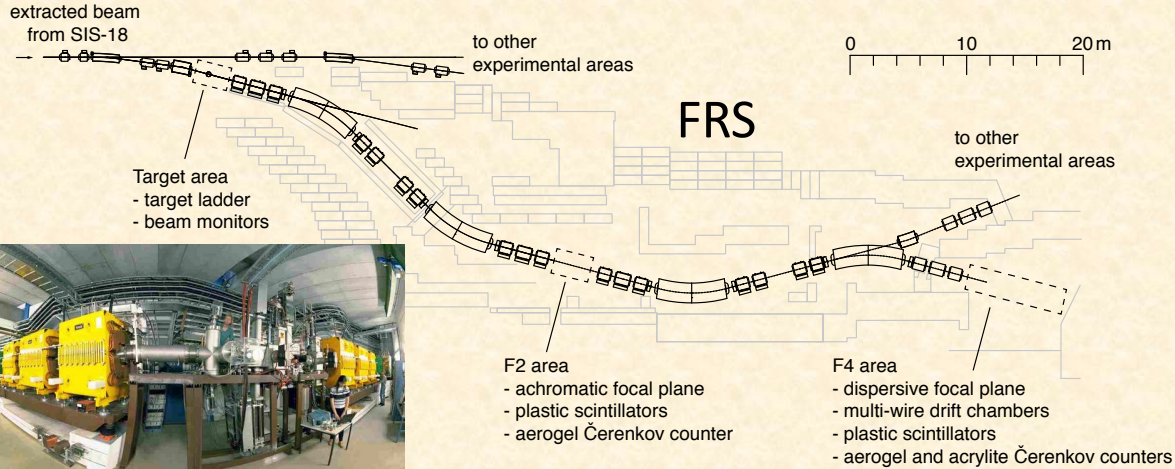
Measurement of fragmentation cross section up to 2 A GeV

GSI/FAIR in Germany

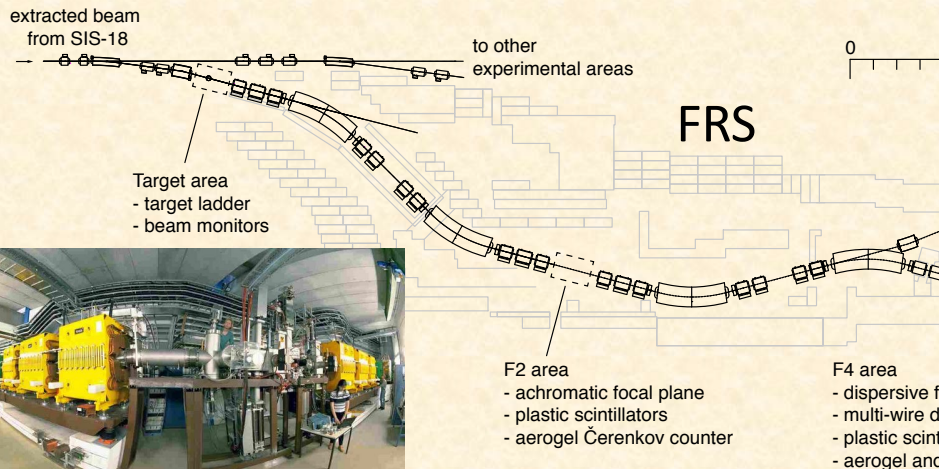


Including unstable nuclear beams

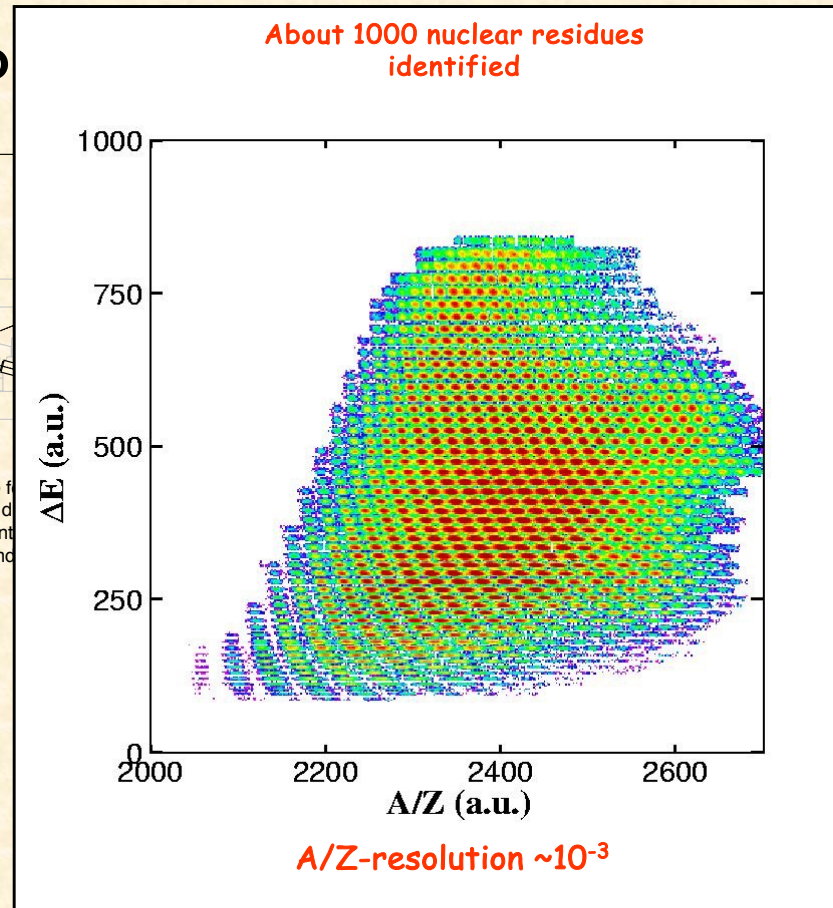
Measurement of fragmentation cross section up to 2 A GeV



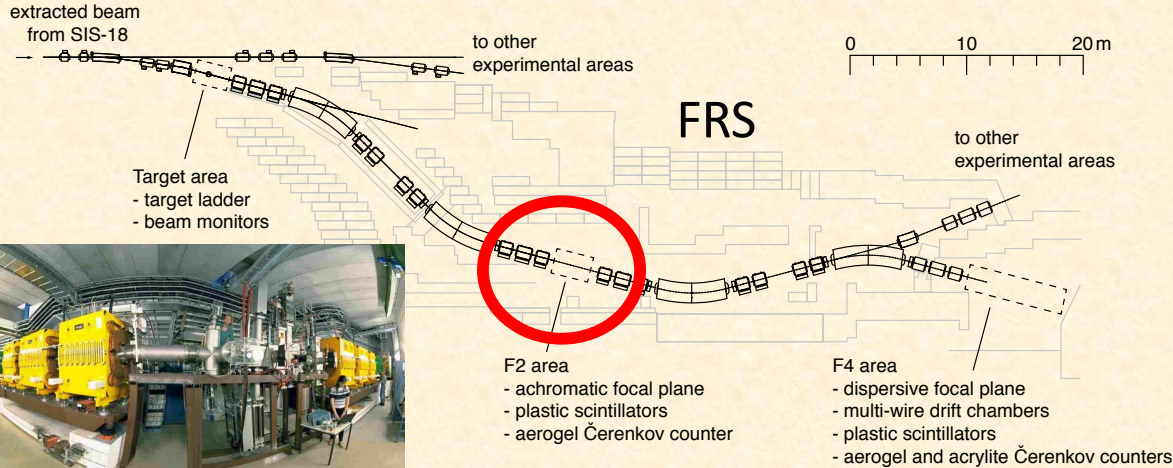
Measurement of fragmentation cross



Analysis of the existing data

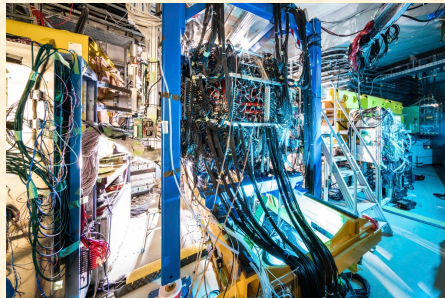


Measurement of fragmentation cross section up to 2 A GeV



WASA-FRS setup

Measuring nuclei, baryons and mesons
(especially protons, pions and kaons)



Exclusive fragmentation reaction
cross section for different final
states

- $^{12}\text{C} + \text{H} \rightarrow \text{X}$
- $^{14}\text{N} + \text{H} \rightarrow \text{X}$
- $^{16}\text{O} + \text{H} \rightarrow \text{X}$
- $^{16}\text{O} + \text{He} \rightarrow \text{X}$
- $^{28}\text{Si} + \text{H} \rightarrow \text{X}$
- $^{11}\text{B} + \text{H} \rightarrow \text{X}$
- $^{12}\text{C} + \text{He} \rightarrow \text{X}$
- $^{24}\text{Mg} + \text{H} \rightarrow \text{X}$
- $^9\text{Be} + \text{H} \rightarrow \text{X}$
- $^{10}\text{Be} + \text{H} \rightarrow \text{X}$
- $\text{Ne, Mg, Si, Fe} \rightarrow \text{Li, Be, B}$

0.5 A GeV – 2.0 A GeV

Developing a robust nuclear fragmentation model/theory
up to 2 A GeV

WASA magnet upgrade is important

- 1 T \rightarrow 2 T
- Electric cooling

Improvement for studying

- Hypernuclei
- Mesic-nuclei and -atoms
- Baryon resonances in exotic nuclei

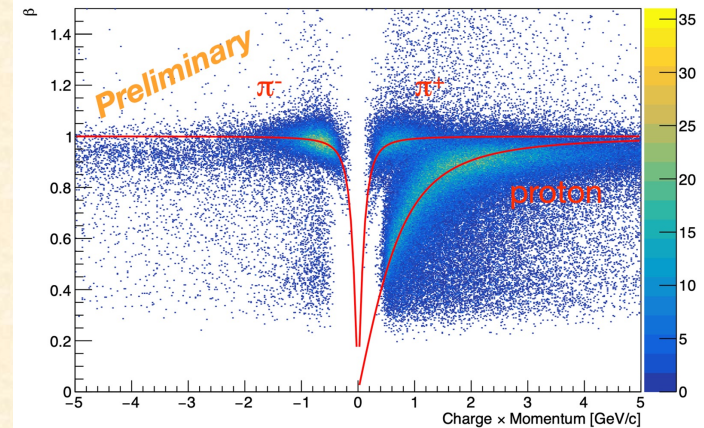
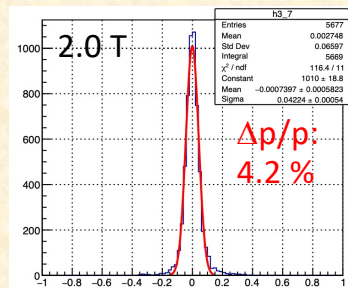
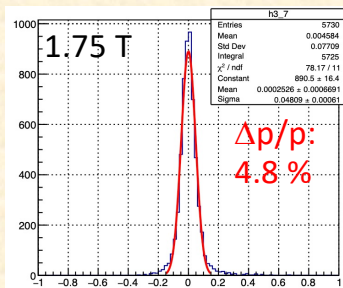
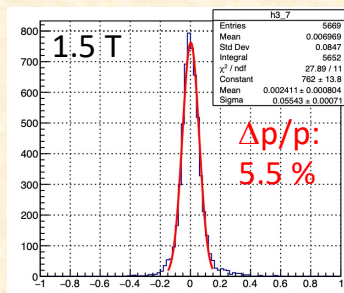
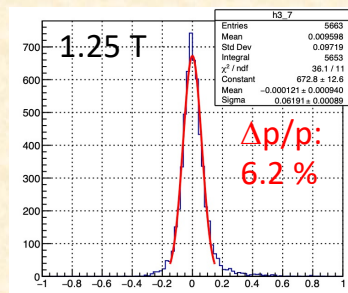
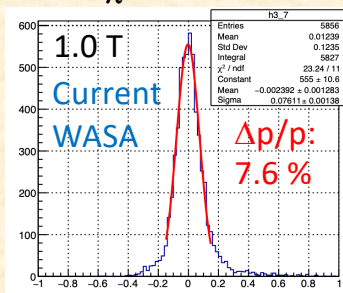
Also opening new opportunities for studying

- **Example:** Nuclear fragmentation reaction
 - To understand the structure of the galaxy
 - To deduce the contribution to cosmic photons from dark matters
 - To understand the origin of the solar system



Particle ID and Momentum

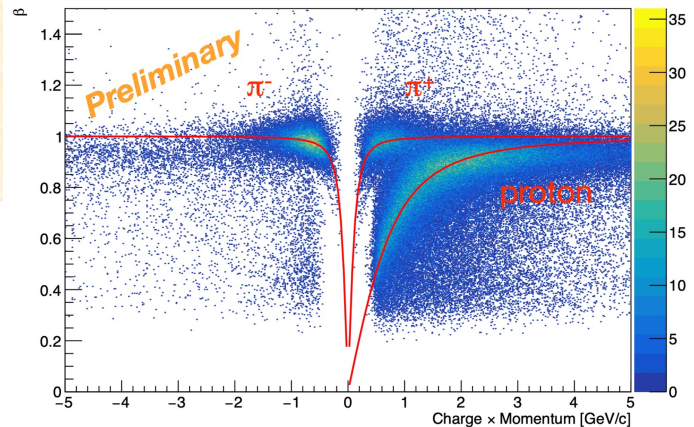
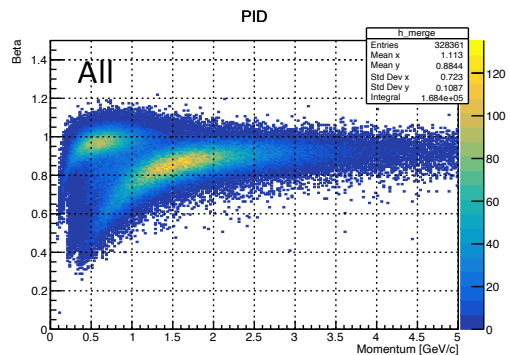
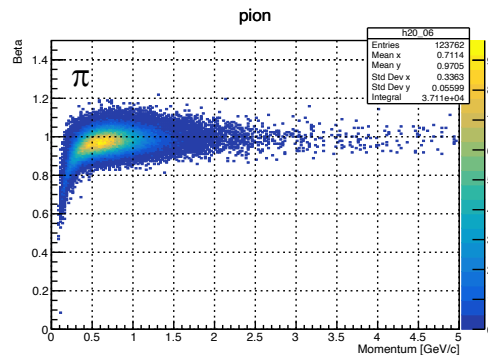
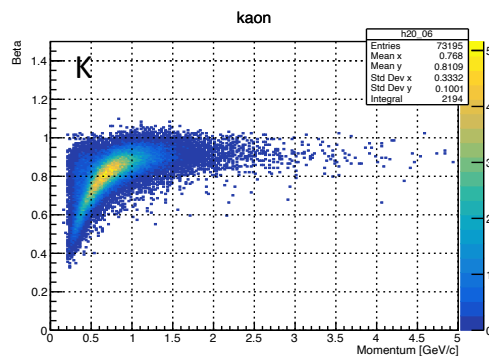
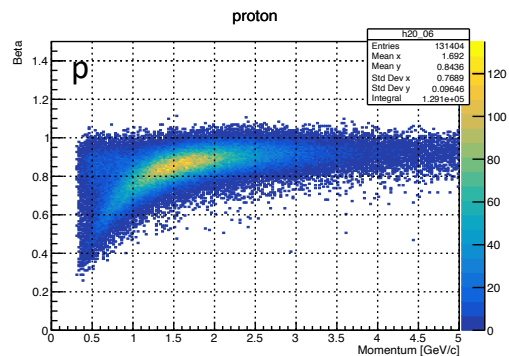
$$P_{\pi} = 0.4 \text{ GeV}/c$$



Particle ID and Momentum

$p:\pi:K = 1:0.3:0.03$

1.0 T

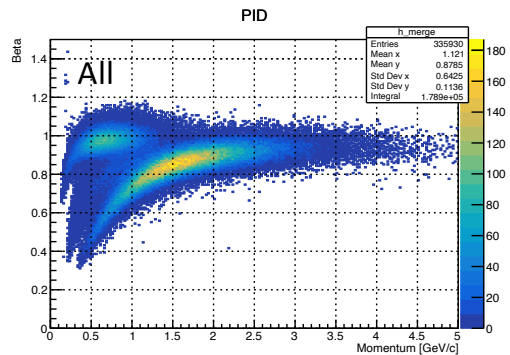
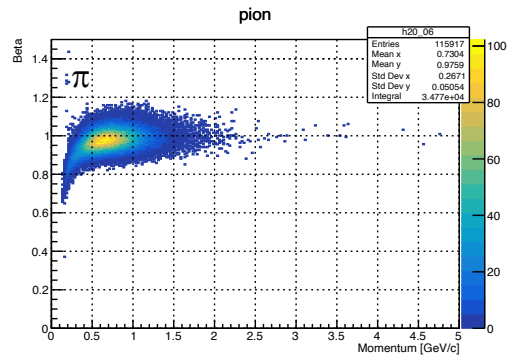
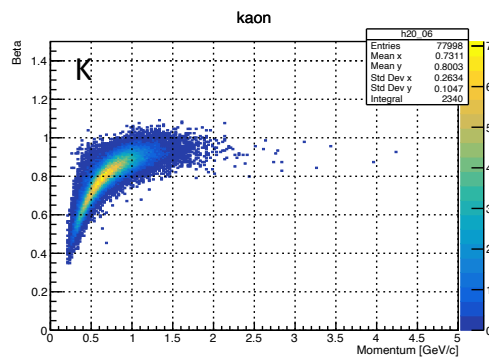
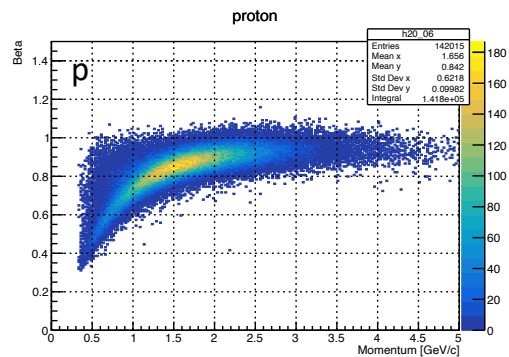
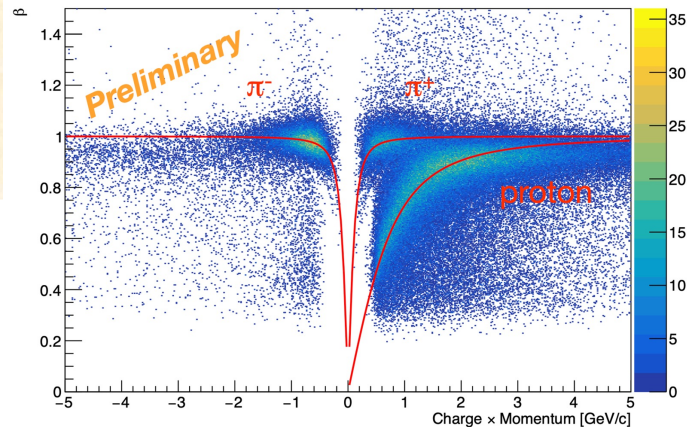


Particle ID and Momentum

$p:\pi:K = 1:0.3:0.03$

2.0 T

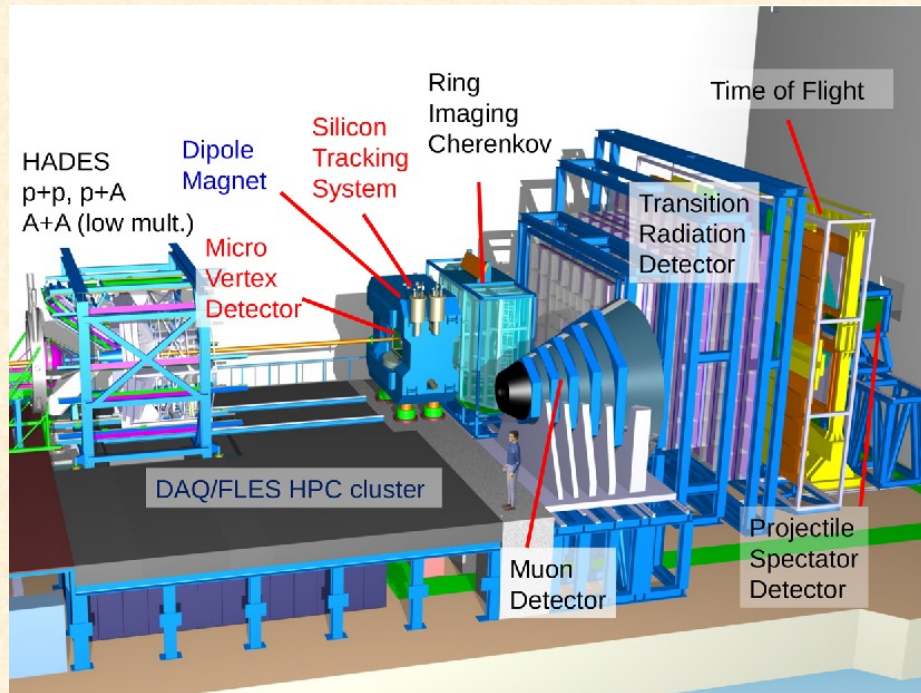
WASA PID (Current 1.0 T)



Measurement of fragmentation cross section above 10 A GeV (Validation of the developed model/theory)

GSI/FAIR in Germany

CBM



Only with stable nuclear beams

Summary

- Information on propagation of energetic cosmic-rays is important for understanding the structure of the galaxy
- Fragmentation of propagating cosmic-rays (nuclei) with an interstellar hydrogen plays an important role

However, the experimental data are poorly precise or missing

- Nuclear physicists should measure fragmentation reaction cross sections precisely
- Our ideas:
 - Exclusive measurement up to 2 A GeV with the WASA-FRS setup at GSI, including fragmentation of rare-isotope beams, in order to develop robust fragmentation reaction theory/model
 - Validate the theory/model by measuring the cross section around at 10 A GeV by using the CBM setup at FAIR